

1

2 **Distinct selection signatures during domestication and improvement in**
3 **crops: a tale of two genes in mungbean**

4

5 Ya-Ping Lin^{1,2#}, Hung-Wei Chen^{1#}, Pei-Min Yeh¹, Shashi S. Anand¹, Jiunn Lin³, Juan
6 Li^{1,4,5}, Thomas Noble⁶, Ramakrishnan Nair⁷, Roland Schafleitner², Maria Samsonova⁸,
7 Eric Bishop-von-Wettberg^{8,9}, Sergey Nuzhdin¹⁰, Chau-Ti Ting¹¹, Robert J. Lawn¹², and
8 Cheng-Ruei Lee^{1,3*}

9

10 1. Institute of Ecology and Evolutionary Biology, National Taiwan University, Taipei
11 10617, Taiwan

12 2. World Vegetable Center Headquarter, Tainan 74199, Taiwan

13 3. Institute of Plant Biology, National Taiwan University, Taipei 10617, Taiwan

14 4. Institute of Ecology and Evolution, University of Bern, Bern, Switzerland

15 5. Swiss Institute for Bioinformatics, Lausanne, Switzerland

16 6. Queensland University of Technology, Brisbane, Australia

17 7. World Vegetable Center South and Central Asia, ICRISAT Campus, Patancheru,
18 Hyderabad, Telangana 502324, India

19 8. Mathematical Biology and Bioinformatics Laboratory, Peter the Great St. Petersburg
20 Polytechnic University, St. Petersburg, Russia

21 9. Department of Plant and Soil Science and Gund Institute for the Environment,
22 University of Vermont, Burlington, VT 05405, USA

23 10. University of Southern California, Los Angeles, CA 90089, USA

24 11. Department of Life Science, National Taiwan University, Taipei 10617, Taiwan

25 12. College of Science & Engineering, James Cook University, Townsville, Queensland
26 4814, Australia

27

28 # Equal contribution

29

30 * *Corresponding author*

31 *Cheng-Ruei Lee*

32 *chengrueilee@ntu.edu.tw*

33

34 **Keywords:** *Vigna radiata*, demographic history, selective sweeps, pod shattering, stem
35 determinacy

36

37

38 **Abstract**

39 Domestication and improvement are two crucial processes underlying the evolution of
40 crops. Domestication transformed wild plants into a utilizable form for humans;
41 improvement refined cultivars adapting to distinct environments and local preferences.
42 Using whole-genome re-sequencing of *Vigna radiata*, we investigated the demographic
43 history and compared the genetic footprints of domestication and improvement. The Asian
44 wild population migrated to Australia at about 50 kya, and domestication happened in Asia
45 about 9 kya selecting for non-shattering pods. The key candidate gene for this trait,
46 *VrMYB26a*, has lower expression in cultivars, consistent with the reduced polymorphism
47 in the promoter region reflecting hard selective sweep. The determinate stems were later
48 selected as an improvement phenotype and associated with the gene *VrDet1*. Two ancient
49 haplotypes reducing gene expression exhibit intermediate frequencies in cultivars,
50 consistent with selection favoring independent haplotypes in soft selective sweep. Our
51 results suggest domestication and improvement may leave different genomic signatures of
52 selection, reflecting the fundamental differences in the two processes and highlighting the
53 limitations of genome-scan methods relying on hard selective sweep.

54

55 **Introduction**

56 Crop evolution encompasses two phases, domestication and improvement (Hufford, et
57 al. 2012; Li, et al. 2013; Meyer and Purugganan 2013; Abbo, et al. 2014; Giovannoni 2018;
58 Kumar, et al. 2021). The former refers to the initiation of the divergence from the wild
59 progenitor. Strong selection occurs upon a small population of wild progenitors, with
60 accompanying loss of genetic and phenotypic diversity. Given that domestication aims to
61 increase human benefits rather than plant fitness in the wild, this process typically leads to
62 the so-called domestication syndrome, including the loss of seed shattering and dormancy,
63 gain of gigantism, and the reduction of lateral branches. For example, teosinte (*Zea mays*
64 ssp. *parvigalumis*), the progenitor of maize, has more lateral branches and a tendency for
65 ear shattering than maize (Doebley, et al. 1995). *Oryza rufipogon*, the progenitor of rice,
66 shows more easily seed shattering and smaller seeds than rice (Huang, Kurata, et al. 2012).
67 Improvement, on the other hand, generally occurred accompanying the spread of the
68 domesticated populations to different agro-ecological regions, primarily focusing on
69 increasing yield and the enhanced adaptation to local environments or cultivation systems.
70 For example, soybean varieties in northern Japan required shorter days to flowering than
71 those in southern Japan, suggesting that the regional farmers selected soybeans according
72 to local environments (Kaga, et al. 2012). Given the different natures of these two selection
73 processes, it is intriguing whether they affected the underlying genes and crop genomes in
74 different ways.

75 Meyer et al. (2013) proposed criteria for defining domestication and improvement genes
76 in crops. Genes controlling domestication traits are supposed to undergo positive selection,
77 and the causal mutations would eventually become nearly fixed in all lineages from a
78 single domestication event (Meyer and Purugganan 2013). For example, *sh4*, the loss-of-
79 function allele of one of the influential domestication genes controlling non-shattering in
80 rice, is almost fixed in cultivated rice (Li, et al. 2006). On the other hand, improvement
81 genes may exhibit different signatures of selection since the target phenotypes for
82 improvement often differ depending on local environments and cultivation systems,
83 diversifying the phenotypes of worldwide varieties (Huang, Zhao, et al. 2012; Zhang, et al.
84 2015). For instance, in soybean, the mutant allele of the flowering-time gene *E1* resulted
85 in the change of photoperiod requirement and was enriched in specific populations,

86 associated with the adaptation of soybean cultivars to diverse environments (Xia, et al.
87 2012; Zhou, et al. 2015). Despite the general knowledge of expected differences between
88 domestication and improvement processes, only few have specifically contrasted their
89 genomic signatures of selection in the same species.

90 *Vigna radiata*, mungbean, a traditional legume crop in Asia, was believed to be
91 originated in India (Purugganan and Fuller 2009). Its putative ancestor, *V. radiata* var.
92 *sublobata*, occupies a wide range from Africa, South Asia, Indonesia, to Australia (Tateishi
93 1996; Castillo and Fuller 2010). Two recent studies used reduced-representation
94 sequencing to investigate the genetic structure of cultivated mungbean (Noble, et al. 2018;
95 Brerria, et al. 2020), but genome-wide investigation comparing the cultivars and wild
96 progenitors is lacking. The genetic architecture of trait differences between wild and
97 cultivar groups were investigated in bi-parental crosses (Isemura, et al. 2012; Li, et al.
98 2018). Some of these traits are classic domesticated traits, such as the loss of pod twisting
99 and seed dormancy, and other traits, such as plant stature and yield components, resulted
100 from the improvement phase (Huyghe 1998; Fuller and Allaby 2018). To investigate the
101 genomic and genetic patterns of domestication and improvement, studies using whole-
102 genome sequencing from many wild and cultivar accessions are required.

103 In this study, we re-sequenced 114 *V. radiata* accessions and investigated demographic
104 histories and origins of distinct wild and cultivar groups. We targeted two genes controlling
105 important domestication and improvement traits, pod twisting and stem determinacy, to
106 elucidate how artificial selections during these two processes shape genetic architecture
107 and leave distinct selection signatures at targeted loci.

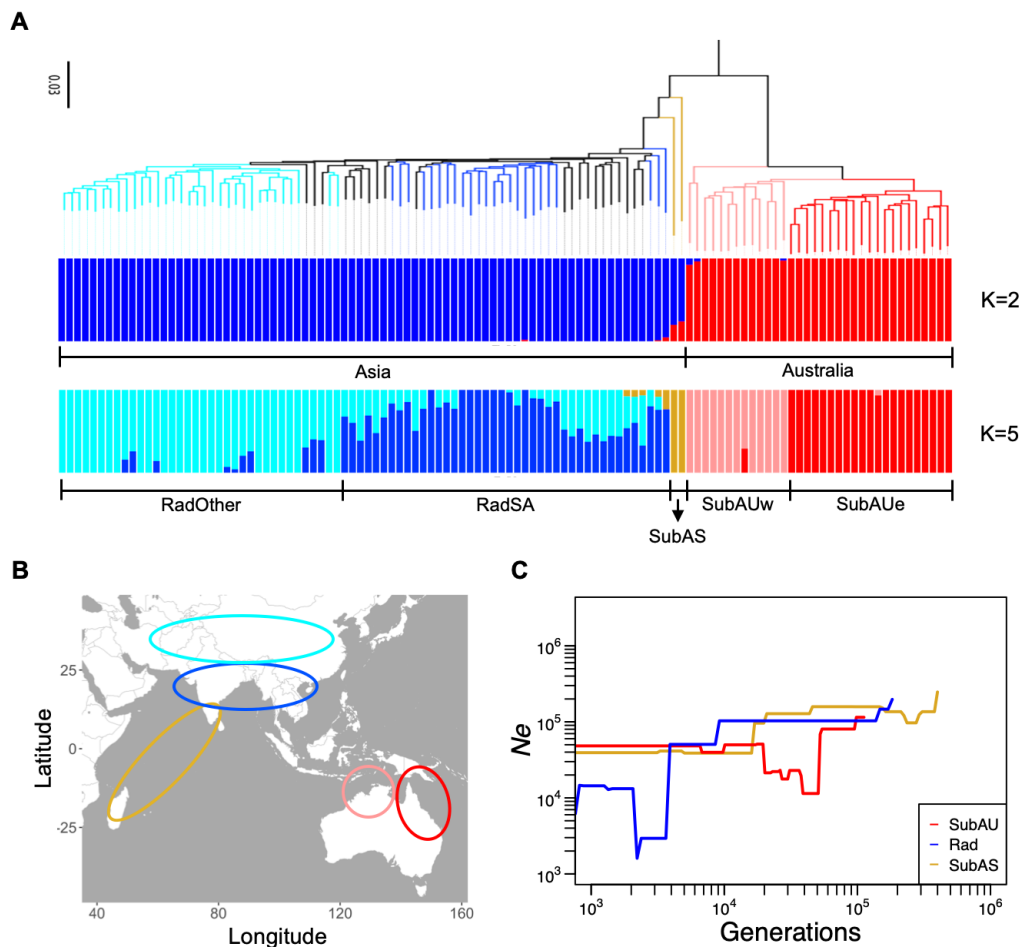
108

109 **Results**

110 **Genetic variation of global *V. radiata***

111 The whole-genome sequencing data were generated for 114 *V. radiata* accessions (36
112 wild and 78 cultivars) and one accession of closely-related species, *V. mungo*. The
113 sequencing depth was $33.52 \pm 9.76X$ per accession. The mapping rate of these raw reads
114 to the *V. radiata* reference genome version 6 was $98.08 \pm 2.67\%$ (Supplementary Table
115 S1). Finally, we identified 18,548,167 (18.5 million) bi-allelic SNPs for the following
116 analyses.

117 We used these SNPs to infer the genetic structure. Lower cross-validation error values
118 of ADMIXTURE exist in $K = 2$ and 5 (Supplementary Fig. S1). Accessions from the same
119 continent were clustered together when $K = 2$ (Figure 1A separating Asia and Australia;
120 Supplementary Table S2). Under $K = 5$, the wild accessions were divided into eastern
121 Australian ones (SubAUe), western Australian ones (SubAUw), and Asian ones (SubAS),
122 and the cultivars were separated into two groups from South Asia (RadSA) and other
123 regions in Asia (RadOther). A similar pattern was observed in the phylogenetic tree and
124 network (Figure 1A-B and Supplementary Fig. S2). The mean F_{ST} value between wild and
125 cultivar populations was 0.49, showing a high degree of differentiation. The wild groups
126 have higher nucleotide diversity than the cultivar groups (Supplementary Fig. S3A).
127 Likewise, LD decays much faster in the wild than in the cultivar population, reaching $r^2 =$
128 0.2 at about 22 kb and 173 kb, respectively (Supplementary Fig. S3B).
129



130 **Figure 1. Population structure and demographic history.** (A) Neighbor-joining
131 phylogenetic tree and population structure of the 114 mungbean accessions. *Vigna mungo*,
132 VI035226, is the outgroup of the phylogenetic tree. (B) Geographic distribution of the
133 inferred genetic groups. (red: SubAUe, pink: SubAUw, goldenrod: SubAS, blue: RadSA,
134 skyblue: RadOther) (C) Inferred demographic history.

135

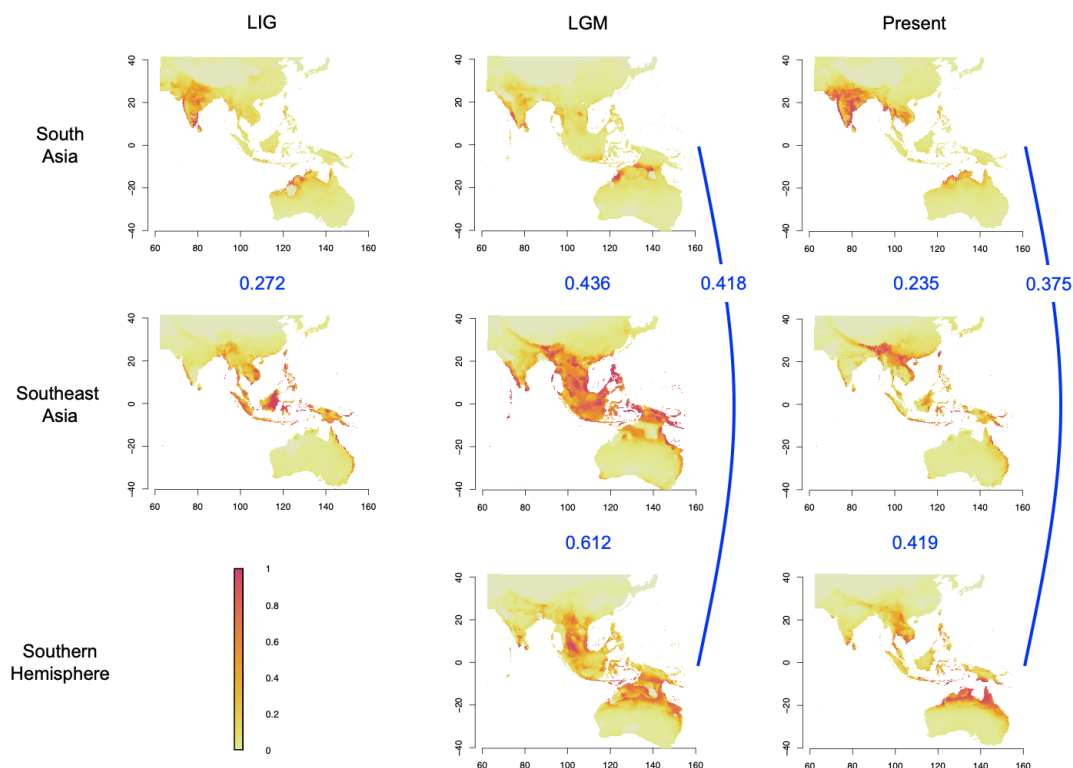
136 **Demographic history**

137 Most species closely related to *V. radiata* exist in Asia (Norihiko, et al. 2010), so
138 mungbean likely has an Asian origin. The existence of many wild accessions in Australia
139 suggests ancient migration from Asia across the Wallace line. We estimated that the Asian
140 and Australian groups first diverged at about 50 thousand years ago (kya) (Figure 1C,
141 Supplementary Fig. S4A-B). After the divergence, the effective population size of SubAU
142 decreased by about tenfold while that of SubAS remained relatively stable, consistent with
143 SubAU being a founder population colonizing Australia. After this major vicariance
144 between Asia and Australia, Asian cultivars (Rad) diverged from SubAS at about 9 kya
145 (Figure 1C, Supplementary Fig. S4C). After the initial domestication, the effective
146 population size of Rad dropped close to 20 times since 4 kya, presumably due to intensified
147 artificial selection and coinciding with archeological records during 4 to 3 kya (Fuller
148 2007). The decreased effective population size of Rad might also be affected by climate
149 change, as 4 kya coincides with the start of climate cooling after the Holocene climate
150 optimum (Marcott, et al. 2013).

151 The strong divergence between Asian and Australian groups was also apparent from the
152 2D site frequency spectrum comparing Rad, SubAUe, and SubAUw (Supplementary Fig.
153 S5). SubAUe and SubAUw had more shared four-fold degenerate SNPs than each of them
154 with Rad, consistent with their closer relationship. On the contrary, SNPs with high impact
155 were enriched in low-frequency derived-allele categories with few shared between
156 populations. These SNP sites were probably under negative selection, and presumably,
157 detrimental ancestral variations were unlikely to be retained in both descendant populations.

158 Our results suggested Australian wild (SubAU) population diverged from the Asian wild
159 group (50 kya) (Figure 1C) during the last ice age (115-11.7 kya), which allows us to track
160 the change in the environmental niche space of these groups. During the last interglacial

161 period (120-140 kya), when *V. radiata* had not colonized Australia, Australia was a less
162 suitable habitat for the Asian groups (Figure 2). During the last ice age, the Sunda Shelf
163 and northern Sahul Shelf were suitable for both the Southeast Asia and Southern
164 Hemisphere populations, facilitating the expansion of *V. radiata* from Southeast Asia into
165 Australia both geographically and environmentally (Figure 2, Supplementary Fig. S6). The
166 Schoener's D values (higher values representing higher niche similarity) also supported that
167 the Southern Hemisphere population shared more suitable habits with the Southeast Asian
168 population (0.612) than the South Asian one (0.418). At present, most of the Malay
169 Archipelago and Australia appear unsuitable for the South and Southeast Asia populations.
170 However, continental Southeast Asia and northern Australia appear suitable for the
171 Southern Hemisphere population.
172



173 **Figure 2. Ecological niche modeling of suitable habitats for the wild mungbean**
174 **populations in South Asia, Southeast Asia, and Southern Hemisphere from the past**
175 **to present.** Colors represent niche suitability. The three rows (South Asia, Southeast Asia,
176 and Southern Hemisphere) represent niche models constructed from the presence data of
177 wild mungbean from these regions and projected to the whole geographical extent. Data of

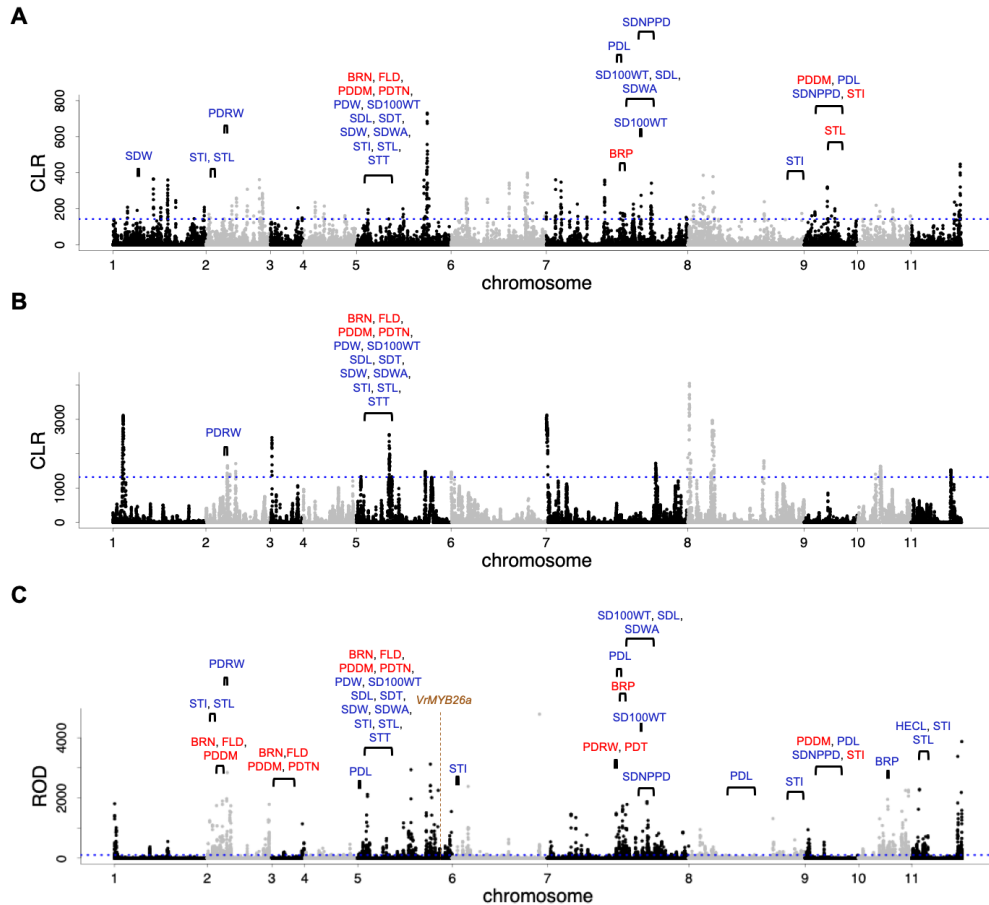
178 Last Interglacial period (120-140 kya, LIG) and the Last Glacial Maximum (22 kya, LGM)
179 were based on the circulation model of MIROC-ESM. The numbers in blue between pairs
180 of modeled distribution indicate the Schoner'D values, where higher values represent
181 higher niche similarity.

182

183 **Selective sweeps in mungbean**

184 We used three approaches to investigate selection footprints across the genome.
185 Potentially selective signals across the genomes of wild and domesticated mungbeans were
186 detected by identifying the regions with the top 1% value in the composite likelihood ratio
187 (CLR) analysis (Figure 3A-B). There were 429 genes detected across the wild genome, and
188 the gene ontology (GO) analysis showed that these genes were significantly enriched in the
189 function of the protein binding and metabolic process (Supplementary Fig. S7A).
190 Comparing our selection scan results to previous QTL mapping explicitly focusing on the
191 divergence between wild and cultivar accessions (Isemura, et al. 2012), the wild accessions'
192 alleles of these QTL generally have more pods, a higher proportion of shattering pods, and
193 smaller seed size.

194



195 **Figure 3. Signatures of selection across the mungbean genome.** Composite likelihood
 196 ratio (CLR) values across the genomes of the (A) wild and (B) domesticated mungbean.
 197 (C) Selective sweeps during domestication inferred from reduction of diversity (ROD)
 198 values. To improve the accuracy, only the QTL with the interval < 15 Mb and overlapped
 199 with selection signals were labeled. The red and blue texts indicate wild or cultivar alleles
 200 have higher trait values in the QTL, respectively. The blue horizontal dashed lines indicate
 201 the cut-off (top 1%) of candidate selective signals. One of the candidate domestication
 202 genes, *VrMYB26a*, was labeled with brown color. (Abbreviation of traits- BRN: branch
 203 number, BRP: position of the first branch, FLD: days to first flower, HECL: hypocotyl plus
 204 epicotyl length, PDDM: days to maturity of the first pod, PDL: pod length, PDRW: rate of
 205 shattered pods, PDT: number of twist of the shattered pod, PDTN: total pod number, PDW:
 206 pod width, SD100WT: 100 seed-weight, SDL: seed length, SDNPPD: number of seeds per
 207 pod, SDT: seed thickness, SDW: seed width, SDWA: seed water absorption, STI: stem
 208 internode length, STL: stem length, STT: stem thickness).

209

210 For cultivated mungbean, the selected regions across the cultivar genome colocalized
 211 with the QTL where the cultivar alleles conferred lower pod dehiscence and fewer pods.

212 There were 420 candidate genes in selected regions, and the GO terms were enriched in
213 carbohydrate binding, response to biotic stimulus, and regulation of nitrogen compound
214 metabolic process (Supplementary Fig. S7B). Notably, legumes are able to form a
215 symbiotic relationship with rhizobia, a unique characteristic involving in nitrogen fixation
216 process (Janczarek, et al. 2015). Thus, enrichment results suggested the important role of
217 mungbean cultivars for soil fertility. This is supported by the first written record of
218 mungbean in an ancient Chinese agricultural literature (齊民要術, Qimin Yaoshu, 544 AD),
219 which emphasized its value as green manure. Other ancient Chinese sources also repeatedly
220 mentioned using mungbean to restore soil fertility in the rotation system (Chen 1980).

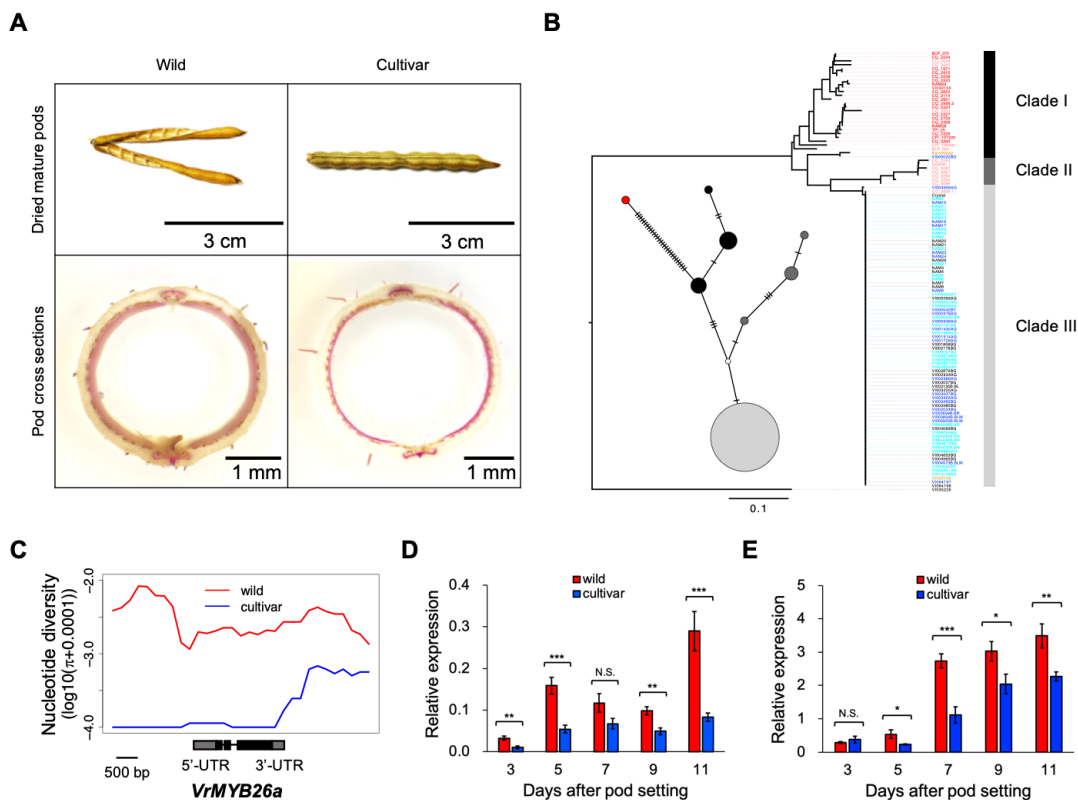
221 A total of 1,232 genes have potential signatures of selective sweeps from the reduction
222 of diversity (ROD) method comparing cultivars relative to wild accessions (Figure 3C).
223 These candidate genes were enriched in GO terms such as catalytic activity, DNA binding,
224 developmental growth, and response to stimulus and chemicals (Supplementary Fig. S7C).
225 Among them, *INVA* is one of the candidate genes responsible for seed size in durum wheat
226 (Mangini, et al. 2021). *ARG1* is the ortholog of the omega-3 fatty acid desaturase gene
227 (*FAD3*), which influences the oil composition in soybean seeds (Bilyeu, et al. 2005; Pham,
228 et al. 2012). *BG7S-2* is likely responsible for basic 7S globulin, one of the storage proteins
229 in mungbean seeds (Mendoza, et al. 2001; Hirano 2021). The high-ROD regions
230 colocalized with the QTL regulating phenology, pod and seed enlargement, pod twisting
231 and dehiscence, and yield. Overall, these results suggested that the wild mungbean was
232 likely under natural selection for dispersal: the wild alleles of these QTL generally have
233 more pods, a higher proportion of shattering pods, and smaller seed size. On the other hand,
234 the cultivars were selected for pod non-shattering as well as pod and seed gigantism, with
235 fewer pods as a potential trade-off.

236

237 ***VrMYB26a* associated with the domestication trait pod non-shattering**

238 In legumes, loss of pod twisting is one of the essential traits during domestication (Fuller
239 and Allaby 2018). Among all the putative domestication genes, *MYB26*, which is involved
240 in pod shattering in *Phaseolus vulgaris*, *Vigna angularis*, and *V. unguiculata* (Takahashi,
241 et al. 2020; Di Vittori, et al. 2021), was detected to be under positive selection in the
242 cultivars (Figure 3C). The thickness of the lignified sclerenchyma layer on the pod walls

243 strongly correlates with the coiling of pod walls (Takahashi, et al. 2020; Parker, et al. 2021).
244 Like other legume species, mungbean cultivars have a thinner lignified layer than wild
245 accessions (Figure 4A). Mungbean has two *MYB26* copies, one on chromosome 5
246 (*VrMYB26a*) and the other on chromosome 9 (*VrMYB26b*). According to the phylogenetic
247 relationship with the other legume homologs, *VrMYB26a* was clustered with the *MYB26*
248 orthologs associated with pod shattering in *P. vulgaris*, *V. angularis*, and *V. unguiculata*
249 (Clade A), and the other clade contained *VrMYB26b* (Clade B) (Supplementary Fig. S8A).
250 The genes in Clade A showed lower d_N/d_S than those in Clade B (Supplementary Fig. S8B),
251 indicating a stronger selection constraint in the former clade. Despite larger difference of
252 allele frequency of three non-synonymous SNPs between wild and cultivars in *VrMYB26a*
253 coding region, the function of its encoding protein is probably not changed due to the
254 similar property of amino acids. (Supplementary Fig. S9). We inferred whether the
255 differential expression, instead of amino acid changes, results in non-twisting pods in
256 cultivars.
257



258 **Figure 4. *VrMYB26a* associated with pod twisting in mungbean.** (A) Mature pods and
 259 pod cross-sections from the wild (NAM30) and cultivated (VI004853) mungbean
 260 accessions. The cross-section's lignin was stained in red. (B) Neighbor-joining tree of
 261 *VrMYB26a* promoter region (upstream 2kb) of 114 mungbean accessions and one *V. mungo*
 262 as outgroup. Accession names are labeled with colors based on population structure (K =
 263 5). Also shown is the haplotype network based on 61 SNPs in the same region, and the
 264 outgroup was labeled with a red dot. Haplotypes were colored based on the clades
 265 identified from the tree. The sizes of circles correspond to the number of individuals in this
 266 haplotype. (C) Patterns of nucleotide diversity in sliding windows (window size, 1 kb; step
 267 size, 0.2 kb) of the wild and cultivar groups from the 2-kb upstream of *VrMYB26a* to its 2-
 268 kb downstream regions. (D) Expression levels of *VrMYB26a* during pod development. (E)
 269 Expression levels of *VrCAD4* during pod development. In (D) and (E), three accessions of
 270 wild and cultivar groups were used, respectively. The data are presented as mean \pm standard
 271 error (N.S. indicates non-significant; *, **, and *** indicate p value < 0.05, 0.01 and 0.001,
 272 respectively).

273

274 The neighbor-joining tree and haplotype network of the *VrMYB26a* promoter region
 275 (upstream 2kb) supported the near-fixation of the derived allele in cultivars (Figure 4B).
 276 Together with the apparent reduction of nucleotide diversity at the upstream of *VrMYB26a*

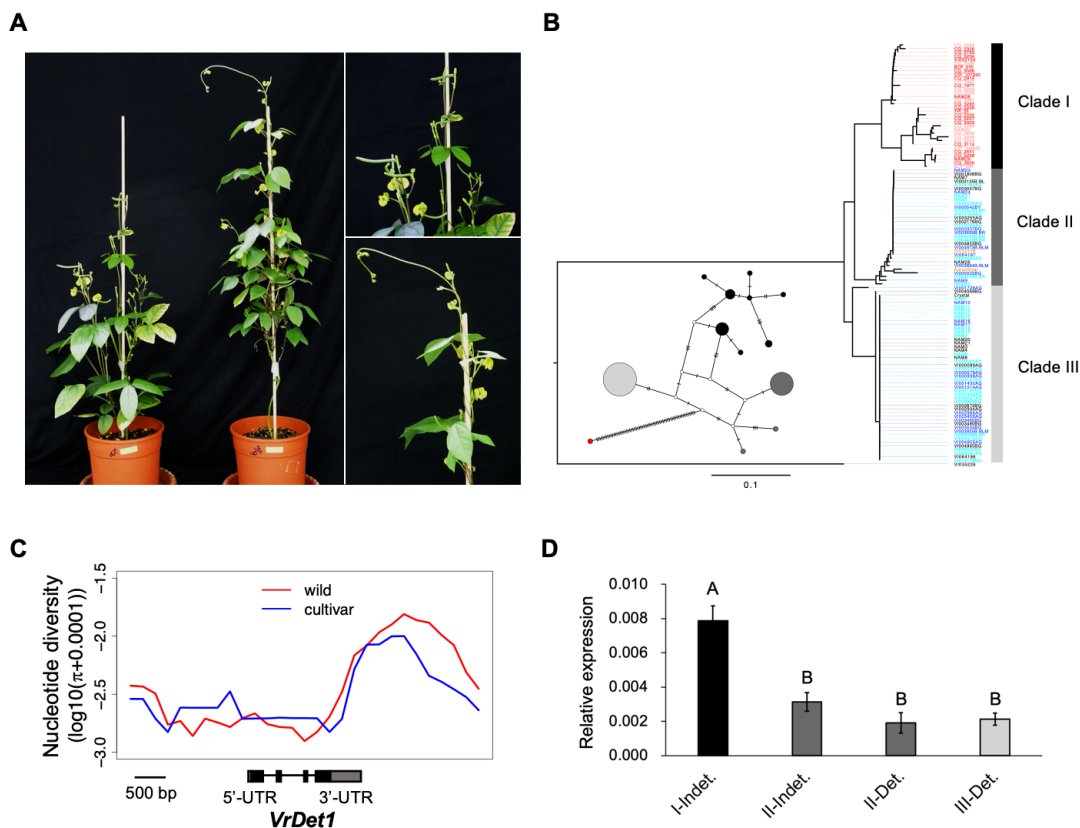
277 in cultivars (Figure 4C), these lines of evidence suggested that the expression pattern of
278 *VrMYB26a* was the likely target of selection for non-twisting pods. We then evaluated the
279 gene expression of *VrMYB26a* during pod development. The wild accessions showed
280 significantly higher expression of *VrMYB26a* than cultivars on average, except on the 7th
281 day after pod setting (DAP) (Figure 4D). Similarly, the expression of *VrCAD4*, a critical
282 downstream gene involved in lignin biosynthesis (Xie, et al. 2018), was significantly higher
283 in wild accessions than cultivars, except on the 3th DAP (Figure 4E). This suggested the
284 lower expression of *VrMYB26a* reduced expression of downstream lignin biosynthesis
285 gene, which contributed to non-twisting pods with thinner sclerenchyma layer. The gene
286 responsible for pod non-shattering, an important trait in mungbean domestication, likely
287 experienced the classic pattern of a hard selective sweep, where most cultivars share the
288 same derived allele with low variation.

289

290 ***VrDet1* associated with the improvement trait stem determinacy**

291 Plant architecture, associated with seed yield and environmental adaptation, is often the
292 target of artificial selection during the improvement phase (Huyghe 1998). Like other
293 legume species, wild mungbeans have indeterminate growth, while many cultivars have
294 determinate growth (Nguyen, et al. 2012; Chauhan and Williams 2018), an improved
295 phenotype advantageous for harvesting due to the shorter reproductive periods (Nair, et al.
296 2020). A previous study has shown that *VrDet1* modulated determinacy (Li, et al. 2018).
297 The phenotypic shift from indeterminate to determinate growth was caused by two single
298 nucleotide substitutions at the -1058 and -14 sites upstream of *VrDet1*, reducing its
299 expression. While the previous study was based on only a few wild and cultivar accessions,
300 our comprehensive sampling identified several cultivars with the indeterminate phenotype
301 (Figure 5A). Thus, we further investigate patterns of polymorphism in this essential gene.

302



303 **Figure 5. Stem determinacy and its relationship with *VrDet1*.** (A) Left: Photographs of
 304 indeterminate and determinate mungbean accessions at the reproductive stage. Upper right:
 305 the enlargement of terminal flowers and pods at the main apical stem in a determinate
 306 accession. Lower right: the enlargement vegetative growth at the main apical stem in an
 307 indeterminate accession. (B) Neighbor-joining tree of the *VrDet1* promoter region
 308 (upstream 2kb) of 114 mungbean accessions and one *V. mungo* as an outgroup. Accession
 309 names are labeled with colors based on population structure ($K = 5$). Also shown is the
 310 haplotype network based on 85 SNPs in the same region, and the outgroup was labeled
 311 with a red dot. Haplotypes were colored based on the clades identified from the tree. The
 312 sizes of circles correspond to the number of individuals in this haplotype. (C) Patterns of
 313 nucleotide diversity in sliding windows (window size, 1 kb; step size, 0.2 kb) of the wild
 314 and cultivar groups from the 2-kb upstream of *VrDet1* to its 2-kb downstream regions. (D)
 315 Expression levels of *VrDet1* in the four groups. Colors represent the clades in (B). The data
 316 are presented as mean \pm standard error ($p < 0.001$. Different letters indicate significant
 317 differences from Tukey's HSD-test).

318

319 Non-synonymous SNPs were not found in the *VrDet1* coding region among cultivars,
 320 suggesting that the polymorphism of determinacy in cultivars was not associated with

321 amino acid changes in this gene (Supplementary Fig. S10). The only two non-synonymous
322 SNPs across all of our samples also have low allele frequency differences between cultivar
323 and wild accessions (Supplementary Fig. S10). The neighbor-joining tree of the putative
324 promoter region of *VrDet1* (upstream 2 kb) showed three distinct clades. All Australian
325 wild (SubAU) accessions were clustered in Clade I, two Asian wild (SubAS) accessions
326 clustered in Clade II, and the cultivars clustered in Clade II and III (Figure 5B). The
327 haplotype of the two causal SNPs in Clade I was T⁻¹⁴/T⁻¹⁰⁵⁸, and that in Clade III was A⁻¹⁴/
328 C⁻¹⁰⁵⁸, respectively corresponding to the typical wild and cultivar forms observed in the
329 previous study (Li, et al. 2018). Interestingly, Clade II represents a novel haplotype, T⁻¹⁴/
330 C⁻¹⁰⁵⁸, with the first site corresponding to the wild but the second corresponding to the cultivar
331 alleles. Among accessions with the Clade II haplotype, the two SubAS accessions and eight
332 cultivars were indeterminate, and 22 out of 30 cultivars showed determinate growth.
333 Almost all cultivars in Clade III showed determinate growth.

334 To test whether Clade II (T⁻¹⁴/C⁻¹⁰⁵⁸) originated from a recent recombination event
335 between the wild Clade I (T⁻¹⁴/T⁻¹⁰⁵⁸) and the “typical cultivar” Clade III (A⁻¹⁴/C⁻¹⁰⁵⁸)
336 haplotypes, in this upstream 2 kb region we identified nine diagnostic SNPs with high allele
337 frequency differences between Clade I and III. We used these SNP sites to polarize the
338 allele frequencies in the newly identified Clade II. Instead of the typical patterns of recent
339 recombinant haplotype, where one side of the Clade-II haplotype would conform to Clade-
340 I and the other correspond to Clade-III major alleles, the allele frequencies of Clade II
341 zigzagged among these SNPs (Supplementary Fig. S11). This suggests that Clade II (T⁻¹⁴/
342 C⁻¹⁰⁵⁸) is an ancient haplotype, which is also supported by the haplotype network where
343 haplotypes in both Clade II and Clade III are closer to the root (Figure 5B). Since the
344 cultivars contained two haplogroups of intermediate frequencies, no obvious lack of
345 variation was observed in cultivars compared to wild accessions (Figure 5C). On the other
346 hand, many accessions within Clade II or Clade III possess identical sequences, suggesting
347 their independent rapid frequency increase (Figure 5B).

348 The gene expression level of *VrDet1* in Clade II and III was significantly lower than
349 that in Clade I (Figure 5D), consistent with their determinate phenotype. Notably, the
350 indeterminate accessions in Clade II did not show significantly higher expression than the
351 determinate accessions in Clade II or Clade III, suggesting *VrDet1* expression might not be

352 the only factor affecting stem determinacy. The results suggested that Clade II (T⁻¹⁴/C⁻¹⁰⁵⁸)
353 may have weaker effects than Clade III (A⁻¹⁴/C⁻¹⁰⁵⁸) and have incomplete penetrance,
354 sometimes allowing other genes to cause the ancestral indeterminate phenotype. This is
355 consistent with Clade II containing one wild (T⁻¹⁴) and one cultivar (C⁻¹⁰⁵⁸) allele in the two
356 SNPs previously shown to affect gene expression (Li, et al. 2018).

357 Taken together, our results suggested that the evolution of the improvement trait, stem
358 determinacy, appears to be more complex than the previously suggested simple model of
359 hard selective sweep from the "typical cultivar" Clade III haplotype (Li, et al. 2018).
360 Instead, the evolution might result from soft sweeps of two ancient haplotypes (Clade II T⁻¹⁴/
361 C⁻¹⁰⁵⁸ and Clade III A⁻¹⁴/C⁻¹⁰⁵⁸) reducing the expression of *VrDet1*, with Clade II showing
362 incomplete penetrance allowing the indeterminate phenotype under certain environmental
363 or genomic contexts.

364

365 Discussion

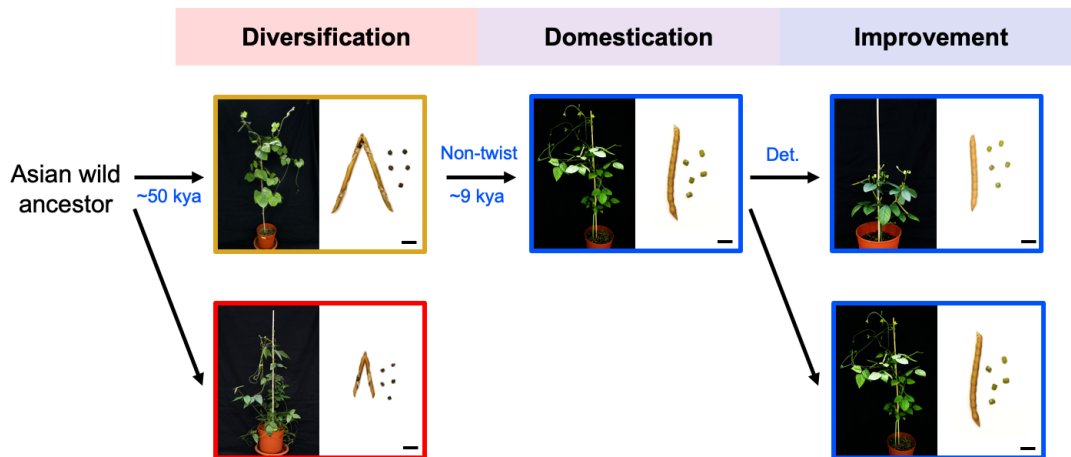
366 In this study, we used whole-genome sequencing to investigate the history of *Vigna*
367 *radiata* before, during, and after domestication. Our results suggest *Vigna radiata*
368 originated in Asia, and the wild population of Southeast Asia likely migrated to Australia
369 during the last ice age. This is supported by the geographical proximity and niche similarity
370 between Southeast Asia and Australia. Domestication probably happened at 9 kya in Asia,
371 after which the cultivars had high selection pressure during domestication for loss of pod
372 shattering to prevent yield loss. Subsequently, some cultivars with determinate shoot
373 growth were selected during improvement. Given the different nature of selection during
374 the domestication and improvement phases, we showed that the candidate genes for these
375 two traits exhibit distinct signatures of selection.

376

377 The evolution of *V. radiata*

378 We proposed a hypothesis of the evolution of *V. radiata*: wild mungbean originated in
379 Asia and migrated into Australia at about 50 kya. This coincides with the initial occupation
380 of Australia by humans (Tobler, et al. 2017), and interestingly, it has been recorded that
381 the tuberous roots of wild mungbean were consumed by Aboriginal Australians (Lawn, et
382 al. 1988). Whether the immigrations of mungbean and human into Australia are associated

383 remains to be further investigated. Compared to their Asian counterparts, wild Australian
384 mungbean evolved smaller seeds (Supplementary Table S3) (Lawn and Rebetzke 2006),
385 likely as an adaptive strategy for dispersal. While wild populations both have twisting pods,
386 the domestication starting at about 9kya further selected for pod non-twisting (Figure 6).
387 Traditional mungbean cultivars were indeterminate (Nair, et al. 2020), and determinate
388 cultivars were further selected during improvement. The phenomenon of two-step artificial
389 selection also occurred in other crops. For example, in rice, seed dormancy and seed
390 shattering were under artificial selection during domestication, while plant height and
391 flowering time were modified locally during improvement (Liu, et al. 2018). The two-step
392 selection in similar traits also occurred in wheat (Roucou, et al. 2018). In tomatoes, yield-
393 related traits were first selected during domestication, and traits of flavor and color were
394 selected in cultivars during improvement (Schouten, et al. 2019).
395



396 **Figure 6. The hypothesis of mungbean evolution.** A wild progenitor of *V. radiata*
397 experienced species diversification, resulting in the divergence of *V. radiata* var. *sublobata*
398 into SubAS (goldenrod box) and SubAU (red box) in about 50 kya. SubAS was further
399 selected for pod non-twisting, becoming *V. radiata* var. *radiata* (blue boxes) during
400 domestication (about 9 kya). Afterwards, some indeterminate cultivars are improved into
401 determinate forms. Bar = 1 cm.

402

403 **Different selection forces resulting in distinct patterns of genetic variation**

404 In legumes, mutations of genes for pod shattering reduce the torsion of pod walls or
405 strengthen the sutures, contributing to non-shattering pods (Parker, et al. 2021). Our result

406 showed that the lower expression of *VrMYB26a* in mungbean cultivars is associated with
407 the thinner sclerenchyma layer in non-twisting pods. In *Vigna angularis* and *V. unguiculata*,
408 it has been shown that mutations creating truncated protein of *MYB26* are likely responsible
409 for non-twisting pods in cultivars (Takahashi, et al. 2020). In *Phaseolus vulgaris*, down-
410 regulation of *PvMYB26* contributed to indehiscent pods (Di Vittori, et al. 2021). These
411 findings reflects Vavilov's Law of Homologous Series in Variation, which stated that
412 parallel evolution in closely-related species often involve genetic changes in homologous
413 genes due to their conserved functions (Vavilov 1922, 1951). In addition, although
414 archeological evidences suggested two possible domestication origins of mungbean from
415 northern and southern India (Fuller and Harvey 2006), only one haplotype was observed in
416 *VrMYB26a* promoter region across all cultivars. We suggested that mungbean likely went
417 through only one domestication event for non-twisting pods. Consistent with the general
418 trend in domestication genes under strong directional selection, we found evidences of hard
419 selective sweep in *VrMYB26a*.

420 As for stem determinacy, indeterminate and determinate growth widely exists in
421 cultivars (Eshed and Lippman 2019). Indeterminate crops have relatively high yields
422 because they provide extended harvest periods and unconstrained canopy development
423 (Chauhan and Williams 2018). Determinate types have short plant height, lodging
424 resistance, and uniform maturity properties (Lawn 1989; Kato, et al. 2019). These two
425 growth habits have different performances under different climate regions or agricultural
426 practices. In the northern regions of America and China, indeterminate soybean varieties
427 are commonly used due to their greater yield under lower temperatures and limited rainfall
428 (Specht, et al. 2014; Kato, et al. 2015; Liu, et al. 2015). In contrast, determinate varieties
429 dominate southern regions (Kilgore-Norquest and Sneller 2000). In mungbean, subsistence
430 farmers prefer cultivating indeterminate varieties for multiple harvesting (Hewavitharane,
431 et al. 2010; Depenbusch, et al. 2021), whereas determinate varieties were commonly used
432 in intensive farming (Nair, et al. 2020). These two types of mungbean cultivars have existed
433 in China since at least the 16th century, as recorded in The Compendium of Materia Medica
434 (本草綱目 Ben Cao Gang Mu, 1578 AD) (Li 2016) and Chinese encyclopedia of
435 technology (天工開物 Tian Gong Kai Wu, 1637 AD) (Song, et al. 1997). The previous

436 study identified alleles (A⁻¹⁴ and C⁻¹⁰⁵⁸) in two SNPs of *VrDet1* responsible for determinate
437 growth in mungbean (Li, et al. 2018). We found that two ancient haplotypes (Clade II T⁻¹⁴/C⁻¹⁰⁵⁸
438 and Clade III A⁻¹⁴/C⁻¹⁰⁵⁸) reduced *VrDet1* expression, suggesting these two
439 haplotypes were selected when determinate varieties were preferred during improvement
440 and consistent with soft selective sweeps (Garud, et al. 2015; Harris, et al. 2018). In
441 soybean, multiple haplotypes of *GmTFL1* associated with determinate growth in soybean
442 were also observed (Liu, et al. 2015). In the cross between two accessions with Clade I and
443 Clade III haplotypes, Li et al. showed perfect co-segregation between determinacy traits
444 and SNP markers in the promoter region (Li, et al. 2018). This suggests the complete
445 penetrance and strong effect of Clade III (A⁻¹⁴/C⁻¹⁰⁵⁸). It's worth noting that some cultivars
446 with Clade II haplotype (T⁻¹⁴/C⁻¹⁰⁵⁸) displayed an indeterminate growth, suggesting this
447 haplotype may have incomplete penetrance allowing the generation of indeterminate
448 phenotype under specific environmental or genomic contexts (Pierce 2012). Under specific
449 environments or agricultural practices where the indeterminate phenotype was preferred,
450 the Clade II haplotype may be favored. In brief, our results showed that multiple adaptive
451 haplotypes of *VrDet1* were selected in mungbean cultivars, resulting in a pattern distinct
452 from the typical signatures of hard selective sweep.

453

454 **Conclusion**

455 In this work, we investigated the evolutionary history of *Vigna radiata* using genomic
456 approaches. Our comparison of phylogenetic tree, haplotype network, and signature of
457 selection at *VrMYB26a* and *VrDet1* loci elucidated distinct genetic architecture behind
458 different phases of artificial selection. For a trait and the relevant gene under selection
459 during the domestication phase, pod twisting and *VrMYB26a* in our case, a hard selective
460 sweep was detected with the near-complete fixation of one derived haplotype in cultivars.
461 For a trait and the relevant gene during the improvement phase, determinacy and *VrDet1*
462 in our case, phenotypic polymorphisms and genetically diverse haplotypes at the locus
463 were observed in cultivars. With whole-genome resequencing of diverse wild and cultivars,
464 we clarify the demographic history of mungbean and revealed distinct patterns of genes
465 affected by artificial selection during crop domestication and improvement phases.

466

467 **Materials and Methods**

468 **Plant materials, library construction, and sequencing**

469 114 *V. radiata* accessions and an outgroup, *V. mungo*, were obtained from two
470 genebanks: the World Vegetable Center in Taiwan and the Australian Grains Genebank
471 (AGG). The passport data from the genebanks provided the taxonomy and country of origin
472 for each accession (Supplementary Table S2). The genomic DNA was extracted from
473 leaves with the DNeasy Plant Mini Kit (QIAGEN). DNA libraries were constructed using
474 NEBNext® Ultra™ II DNA Library Prep Kit for Illumina (E7645), and 150-bp paired-end
475 sequencing was completed using Illumina Hiseq X Ten.

476

477 **Variant calling**

478 Raw sequencing reads were trimmed with SolexaQA++ v3.1.7.1 (Cox, et al. 2010).
479 Then adaptor sequences were removed with cutadapt v1.14 (Martin 2011). The cleaned
480 reads were mapped to the mungbean cultivar (VC1973A) reference genome version 6
481 (Vradiata_ver6) (Kang, et al. 2014) with Burrows-Wheeler aligner v0.7.15 (Li and Durbin
482 2009). Duplicated reads were marked with Picard v2.9.0-1
483 (<http://broadinstitute.github.io/picard/>). Single-nucleotide polymorphisms (SNPs) were
484 called with GATK v3.7 following the GATK Best Practice (McKenna, et al. 2010; Van der
485 Auwera, et al. 2013). We used vcftools v0.1.13 (Danecek, et al. 2011) with following
486 parameters “--min-alleles 2 --max-alleles 2 --remove-indels --max-missing 0.9 --minQ 30”
487 to filter and retain bi-allelic SNPs. For LD decay and fixation index (F_{ST}) analyses, SNPs
488 with minor allele frequency (MAF) < 0.05 were further removed.

489

490 **Gene prediction and annotation**

491 Given that the public gene annotation of *V. radiata* contains only 29,006 genes, which
492 are much less than closely related species (Kang, et al. 2014), we re-annotated the reference
493 genome comprehensively. The whole Vradiata_ver6 genome without masking repeats was
494 annotated ab initio with Augustus v3.3.2 using -species Arabidopsis option (Stanke, et al.
495 2006). For RNAseq evidence, we downloaded RNA sequencing reads from seeds, pods,
496 flowers, and one-week-old and four-week-old whole plants (Chen, et al. 2015; Liu, et al.
497 2016). These RNA reads were mapped onto the Vradiata_ver6 genome with HISAT v2.1.0

498 (Kim, et al. 2015) and assembled and merged by StringTie v1.3.5 (Pertea, et al. 2015). We
499 then blasted the assembled transcripts using blastp v2.8.2 (Camacho, et al. 2009) on the
500 UniProt database (<https://www.uniprot.org/>) and predicted Open Reading Frames using
501 TransDecoder v5.5.0 (Haas, et al. 2013). For protein evidence, the *Glycine max* protein
502 sequences (Wm82.a2.v1) (<https://soybase.org/>) were used as reference protein evidence
503 and aligned to the *Vradiata_ver6* genome with exonerate v2.4 (Slater and Birney 2005). All
504 these evidences were submitted to Evidencemodeler v1.1.1 (Haas, et al. 2008) to identify
505 consensus gene models. The weight of evidence was five except for ab initio evidence,
506 which was one. Finally, the consensus gene models were blasted in the databases of
507 TRAPID (http://bioinformatics.psb.ugent.be/trapid_02/), eggNOG-mapper (Huerta-Cepas,
508 et al. 2017), and plaza (Van Bel, et al. 2018) for functional annotation.

509

510 **Niche modeling**

511 We used the occurrence data of *V. radiata* var. *sublobata* based on the Global
512 Biodiversity Information Facility (GBIF; <https://www.gbif.org/>) and also the collection
513 sites of the wild samples from the Australian Grains Genebank (AGG) and National Bureau
514 of Plant Genetic Resources (NBPGR) to identify the niche of the wild mungbean. The
515 species distribution ranged from 32.927146° N, 66.501760° E to 27.820616° S,
516 155.770869° E. To avoid the over-represented occurrence in a single geographic grid, we
517 removed the overlapped occurrence in the combined data, resulting in 22, 26, and 39
518 samples in South Asia, Southeast Asia, and Southern Hemisphere, respectively
519 (Supplementary Table S4). Nineteen bioclimatic variables, including the current data
520 (1960-1990) and the paleoclimatic data, were downloaded in the highest resolution from
521 WorldClim 1.4 version (<https://www.worldclim.org/data/v1.4/worldclim14.html>). The
522 paleoclimatic data refers to the periods of the Last Glacial Maximum (LGM: 22,000 years
523 ago) under the MIROC-ESM and CCSM4 models, and the Last interglacial (LIG: 120,000-
524 140,000 years ago) under the MIROC-ESM model. After removing the highly correlated
525 bioclimatic variables (Pearson's correlation), we kept six bioclimatic variables in the niche
526 modeling, including BIO1, BIO2, BIO3, BIO12, BIO15, and BIO18, after removing the
527 highly correlated bioclimatic variables (Pearson's correlation coefficients > 0.8). The niche

528 modeling and projection were performed with MaxEnt v3.4.3 using default settings
529 (Phillips, et al. 2006).

530

531 **Population genomics**

532 We inferred population structure with ADMIXTURE v1.3 (Alexander, et al. 2009). An
533 accession was defined as admixed if none of its single ancestral components was more than
534 0.7. The neighbor-joining tree was constructed with TASSEL v5.0 (Bradbury, et al. 2007)
535 and plotted with Figtree v1.4.4 (<http://tree.bio.ed.ac.uk/software/figtree/>). Nucleotide
536 diversity (π) and fixation index (F_{ST}) were calculated using vcftools v0.1.13 (Danecek, et
537 al. 2011). Linkage disequilibrium (LD) between SNPs was calculated with PopLDdecay
538 v3.41 (Zhang, et al. 2019). To examine the relationship among populations, we estimated
539 the genetic distance of 115 accessions with a bi-allelic SNP dataset using Plink v1.90b4.5
540 (--distance) (Purcell, et al. 2007) and then constructed a phylogenetic network with the
541 neighbor-net algorithm in SplitsTree v5.3 (Huson and Bryant 2006).

542

543 **Demographic history**

544 We reconstructed the demographic history of *V. radiata* with SMC++ v1.15.2 (Terhorst,
545 et al. 2017) since this algorithm accepts many samples for a population. Since such an
546 algorithm treats two gene copies within a diploid individual as two randomly sampled
547 haplotypes from the populations and *V. radiata* is a self-fertilizing species, we followed
548 common practices for species like *Arabidopsis thaliana* and soybean (Alonso-Blanco, et
549 al. 2016; Kim, et al. 2021). We generated artificial diploids by assembling haplotypes from
550 two random accessions, except for the admixed accessions, including two wild accessions
551 (NAM30, CPI_106935) and one cultivar (VI005022BG). In addition, the heterochromatic
552 regions, which were defined by regions enriched in repetitive sequences in the
553 *Vradiata_ver6* genome, were excluded. We estimated the divergence time among
554 cultivated *V. radiata* var. *radiata*, the wild group from Australia (SubAU), and the wild
555 group from Asia (SubAS), assuming one generation per year with a mutation rate at 1×10^{-8}
556 (von Wettberg, et al. 2018). We annotated potential effects of SNPs with SnpEff v4.3t
557 (Cingolani, et al. 2012), and SNPs annotated as high or low impacts were used to generate
558 unfolded 2D Site Frequency Spectrum (2D SFS) using *V. mungo* as the outgroup.

559

560 **Detection of selective sweeps**

561 Admixed accessions between wild and cultivar groups were removed from the analyses
562 of selection signals during domestication. Reduction of diversity (ROD; $\pi_{\text{wild}}/\pi_{\text{cultivar}}$) was
563 calculated in 10-kb windows with a 1-kb step size. A composite likelihood ratio (CLR) test
564 was performed with SweeD v4.0.0 (Pavlidis, et al. 2013) in non-overlapping 10-kb sliding
565 windows across the genome. Quantitative trait loci (QTL) of the domestication traits were
566 detected based on previous research (Isemura, et al. 2012) by anchoring their linked
567 markers to the reference genome. Gene ontology (GO) enrichment of the genes under
568 selection was estimated using TBtools v1.098 (Chen, et al. 2020).

569

570 **Phenotyping**

571 The mungbean plants were grown in a growth chamber under 12 hours (30°C) light/ 12
572 hours (25°C) dark at 700 $\mu\text{mol m}^{-2} \text{s}^{-1}$ of light. For stem determinacy, accession was
573 defined as determinate when apical meristems stopped growing soon after flowering. For
574 pod twisting, pods from wild and cultivar accessions were dried in an oven at 37°C for four
575 days before phenotyping. The weight of 100 seeds was the average of three plants in each
576 accession. The number of seeds per pod and pod length was the average of 30 pods (10
577 pods per plant, a total of 3 plants) of each accession.

578 The sclerenchyma tissues, which contain the lignified cell walls, were observed with
579 phloroglucinol–HCl solution (Pomar, et al. 2002). We collected fresh mature pods for
580 histological staining. The phloroglucinol–HCl solution was prepared by dissolving 0.2 g
581 phloroglucinol in 20 ml ethanol and additional 20 ml 37% hydrochloric acid. The free-hand
582 cross-sections of pods were obtained with a razor blade (Corrux) and incubated in
583 phloroglucinol–HCl solution for one minute. We observed the stained slides under an
584 optical dissecting microscope (SZ61; Olympus).

585

586 **RNA isolation and real-time qPCR for *MYB26* and *VrDet1***

587 To detect *MYB26* gene expression during pod development, we collected pods 3, 5, 7,
588 9, and 11 days after pod setting (DAP). Seeds were manually removed except pods at 3 and
589 5 DAP (seeds were too small). A total of 50 mg pod tissues per sample were ground with

590 liquid nitrogen in a 1.5-ml microcentrifuge tube and treated with 65 °C 1.2 ml CTAB buffer
591 (2% CTAB, 1% polyvinylpyrrolidone 40, 2 M sodium chloride, 100 mM Tris-HCl, 20 mM
592 ethylenediaminetetraacetic acid, 2% beta-mercaptoethanol in nuclease-free water) (Wang
593 and Stegemann 2010). The samples were then incubated in a water bath at 65 °C for 30
594 minutes and centrifuged at 1,6000 g for 15 minutes. The supernatant was transferred to two
595 new microcentrifuge tubes and added equal volumes of UltraPure™
596 phenol:chloroform:isoamyl alcohol (25:24:1, Invitrogen). Afterward, the evenly-mixed
597 samples were centrifuged at 1,6000 g for 15 minutes. The supernatant was transferred to a
598 new microcentrifuge tube and mixed with equal volumes of 8M LiCl. Subsequently, the
599 samples were kept in a -20 °C refrigerator for at least 2 hours and then centrifuged at 1,6000
600 g for 30 minutes to remove the supernatant. The pellet was washed with 1 ml 80% ethanol
601 and centrifuged at 1,6000 g for 10 minutes. Finally, the pellet was dissolved in 50 µl
602 nuclease-free water.

603 As for the *VrDet1*, we evaluated the expression using apical meristem at the V0 stage
604 (unifoliate leaves are fully expanded, and the first trifoliate leaves just emerged) following
605 the previous study (Li, et al. 2018). RNA was extracted using the total RNA isolation kit
606 (Novelgene; Cat. No. RT0300). The extracted RNA solution was treated with DNase I
607 (NEB) and then cleaned up with the LiCl method mentioned above.

608 cDNA was synthesized from 1 µg of total RNA for each sample using SuperScript IV
609 Reverse Transcriptase (Invitrogen) and then diluted at 1:20. The iQ SYBR Green Supermix
610 (Bio-Rad) was used to perform real-time qPCR. mRNA's relative expression was
611 calculated using the $2^{-\Delta\Delta CT}$ method (Livak and Schmittgen 2001) using the housekeeping
612 gene *VrCYP20* (Li, et al. 2015). The intron-spanning primers were designed for the qPCR
613 experiment (Supplementary Table S5).

614

615 **Evolutionary and association analyses**

616 We used the coding sequence of *VrMYB26* (LOC106761638) to retrieve its homologous
617 genes in azuki bean (*V. angularis*), cowpea (*V. unguiculata*), common bean (*Phaseolus*
618 *vulgaris*), and *Arabidopsis thaliana* from public databases, including VigGS (Sakai, et al.
619 2016), Phytozome (Goodstein, et al. 2012), and TAIR (Huala, et al. 2001). Sequences were
620 aligned, and the maximum-likelihood (ML) tree was constructed with 1,000 bootstrap

621 replications using MEGA v11(Tamura, et al. 2021). In addition, we estimated pairwise
622 d_N/d_S ratios in each clade according to the Yang & Nielsen (2000) method (Yang and
623 Nielsen 2000) with PAML v4.9 (Yang 2007). We constructed neighbor-joining tree of
624 promoter region of targeted genes with ape package in R v4.1.2 (Paradis and Schliep 2018).
625 The haplotype network was constructed using PopART v1.7 with the TCS algorithm
626 (Leigh and Bryant 2015). We used the SNPs without heterozygotes and missing values in
627 the *VrDet1* and *VrMYB26a* promoter regions for the haplotype network analysis and used
628 *V. mungo* as the outgroup.

629

630 **Acknowledgments**

631 We thank Chia-Yu Chen, Pei-Wen Ong, and Jo-Wei Hsieh for the assistance in sample
632 preparation. We are grateful to the support from National Taiwan University's Computer
633 and Information Networking Center for high-performance computing facilities as well as
634 Technology Commons of College of Life Science for molecular biology assistance. C.-R.L.
635 was funded by 107-2923-B-002-004-MY3 and 110-2628-B-002-027 from the Ministry of
636 Science and Technology, Taiwan. C.-T.T. was funded by 107-2923-B-002-004-MY3 from
637 the Ministry of Science and Technology, Taiwan. Y.-P.L. was supported by 110-2313-B-
638 125-001-MY3 from the Ministry of Science and Technology, Taiwan. R.N. and R.S. were
639 funded by the Australian Center for International Agricultural Research (ACIAR) through
640 the projects on International Mungbean Improvement Network (CIM-2014-079 and
641 CROP-2019-144) and by the strategic long-term donors to the World Vegetable Center:
642 Republic of China (Taiwan), UK aid from the UK government, United States Agency for
643 International Development (USAID), Germany, Thailand, Philippines, Korea, and Japan.
644 E.B.-v.-W. was supported by USDA Multistate Hatch NE1710. M.S. was supported by the
645 Ministry of Science and Higher Education of the Russian Federation under the strategic
646 academic leadership program "Priority 2030" (Agreement 075-15-2021-1333 dated
647 30.09.2021). S.N. was supported by the Zumberge foundation.

648

649 **Author Contributions**

650 C.-R.L. designed and supervised the study. Y.-P.L., H.-W.C., and C.-R.L. performed data
651 analyses and wrote the manuscript with help from other authors. H.-W.C. and P.-M.Y.
652 collected phenotypic data and conducted qPCR experiment. All authors read and approved
653 the manuscript.

654

655 **Data Availability**

656 The raw sequencing data for each of 114 *Vigna radiata* accessions and 1 *V. mungo*
657 generated in this study have been submitted to the NCBI BioProject database
658 (<https://www.ncbi.nlm.nih.gov/bioproject/>) under accession number PRJNA838242.

659

660

661 **References**

- 662 Abbo S, van-Oss RP, Gopher A, Saranga Y, Ofner I, Peleg Z. 2014. Plant domestication
663 versus crop evolution: a conceptual framework for cereals and grain legumes. *Trends in*
664 *plant science* 19:351-360.
- 665 Alexander DH, Novembre J, Lange K. 2009. Fast model-based estimation of ancestry in
666 unrelated individuals. *Genome Res* 19:1655-1664.
- 667 Alonso-Blanco C, Andrade J, Becker C, Bemm F, Bergelson J, Borgwardt KM, Cao J,
668 Chae E, Dezaan TM, Ding W. 2016. 1,135 genomes reveal the global pattern of
669 polymorphism in *Arabidopsis thaliana*. *Cell* 166:481-491.
- 670 Bilyeu K, Palavalli L, Sleper D, Beuselinck P. 2005. Mutations in soybean microsomal
671 omega-3 fatty acid desaturase genes reduce linolenic acid concentration in soybean seeds.
672 *Crop Science* 45:1830-1836.
- 673 Bradbury PJ, Zhang Z, Kroon DE, Casstevens TM, Ramdoss Y, Buckler ES. 2007.
674 TASSEL: software for association mapping of complex traits in diverse samples.
675 *Bioinformatics* 23:2633-2635.
- 676 Breria CM, Hsieh CH, Yen J-Y, Nair R, Lin C-Y, Huang S-M, Noble TJ, Schafleitner R.
677 2020. Population structure of the world vegetable center mungbean mini core collection
678 and genome-wide association mapping of loci associated with variation of seed coat luster.
679 *Tropical Plant Biology* 13:1-12.
- 680 Camacho C, Coulouris G, Avagyan V, Ma N, Papadopoulos J, Bealer K, Madden TL. 2009.
681 BLAST+: architecture and applications. *BMC bioinformatics* 10:1-9.
- 682 Castillo C, Fuller DQ. 2010. Still too fragmentary and dependent upon chance? *Advances*
683 *in the study of early Southeast Asian archaeobotany. Fifty years of archaeology in*
684 *Southeast Asia: Essays in honour of Ian Glover*:91-111.
- 685 Chauhan YS, Williams R. 2018. Physiological and agronomic strategies to increase
686 mungbean yield in climatically variable environments of Northern Australia. *Agronomy*
687 8:83.
- 688 Chen C, Chen H, Zhang Y, Thomas HR, Frank MH, He Y, Xia R. 2020. TBtools: an
689 integrative toolkit developed for interactive analyses of big biological data. *Molecular plant*
690 13:1194-1202.
- 691 Chen H, Wang L, Wang S, Liu C, Blair MW, Cheng X. 2015. Transcriptome sequencing
692 of mung bean (*Vigna radiata* L.) genes and the identification of EST-SSR markers. *PLoS*
693 *one* 10:e0120273.
- 694 Chen L-T. 1980. A study of the systems of rotating crops in Chinese history. *Bulletin of*
695 *the Institute of History and Philology* 51:281-313.
- 696 Cingolani P, Platts A, Wang le L, Coon M, Nguyen T, Wang L, Land SJ, Lu X, Ruden DM.
697 2012. A program for annotating and predicting the effects of single nucleotide
698 polymorphisms, SnpEff: SNPs in the genome of *Drosophila melanogaster* strain w1118;
699 iso-2; iso-3. *Fly (Austin)* 6:80-92.

700 Cox MP, Peterson DA, Biggs PJ. 2010. SolexaQA: At-a-glance quality assessment of
701 Illumina second-generation sequencing data. *BMC bioinformatics* 11:485.

702 Danecek P, Auton A, Abecasis G, Albers CA, Banks E, DePristo MA, Handsaker RE,
703 Lunter G, Marth GT, Sherry ST, et al. 2011. The variant call format and VCFtools.
704 *Bioinformatics* 27:2156-2158.

705 Depenbusch L, Farnworth CR, Schreinemachers P, Myint T, Islam MM, Kundu ND, Myint
706 T, San AM, Jahan R, Nair RM. 2021. When Machines Take the Beans: Ex-Ante
707 Socioeconomic Impact Evaluation of Mechanized Harvesting of Mungbean in Bangladesh
708 and Myanmar. *Agronomy* 11:925.

709 Di Vittori V, Bitocchi E, Rodriguez M, Alseekh S, Bellucci E, Nanni L, Gioia T, Marzario
710 S, Logozzo G, Rossato M. 2021. Pod indehiscence in common bean is associated with the
711 fine regulation of PvMYB26. *Journal of experimental botany* 72:1617-1633.

712 Doebley J, Stec A, Gustus C. 1995. teosinte branched1 and the origin of maize: evidence
713 for epistasis and the evolution of dominance. *Genetics* 141:333-346.

714 Eshed Y, Lippman ZB. 2019. Revolutions in agriculture chart a course for targeted
715 breeding of old and new crops. *science* 366:eaax0025.

716 Fuller DQ. 2007. Contrasting patterns in crop domestication and domestication rates:
717 recent archaeobotanical insights from the Old World. *Annals of Botany* 100:903-924.

718 Fuller DQ, Allaby R. 2018. Seed dispersal and crop domestication: shattering, germination
719 and seasonality in evolution under cultivation. *Annual Plant Reviews online*:238-295.

720 Fuller DQ, Harvey EL. 2006. The archaeobotany of Indian pulses: identification,
721 processing and evidence for cultivation. *Environmental archaeology* 11:219-246.

722 Garud NR, Messer PW, Buzbas EO, Petrov DA. 2015. Recent selective sweeps in North
723 American *Drosophila melanogaster* show signatures of soft sweeps. *PLoS genetics*
724 11:e1005004.

725 Giovannoni J. 2018. Tomato multiomics reveals consequences of crop domestication and
726 improvement. *Cell* 172:6-8.

727 Goodstein DM, Shu S, Howson R, Neupane R, Hayes RD, Fazo J, Mitros T, Dirks W,
728 Hellsten U, Putnam N. 2012. Phytozome: a comparative platform for green plant genomics.
729 *Nucleic acids research* 40:D1178-D1186.

730 Haas BJ, Papanicolaou A, Yassour M, Grabherr M, Blood PD, Bowden J, Couger MB,
731 Eccles D, Li B, Lieber M. 2013. De novo transcript sequence reconstruction from RNA-
732 seq using the Trinity platform for reference generation and analysis. *Nature protocols*
733 8:1494-1512.

734 Haas BJ, Salzberg SL, Zhu W, Pertea M, Allen JE, Orvis J, White O, Buell CR, Wortman
735 JR. 2008. Automated eukaryotic gene structure annotation using EvidenceModeler and the
736 Program to Assemble Spliced Alignments. *Genome biology* 9:1-22.

737 Harris AM, Garud NR, DeGiorgio M. 2018. Detection and classification of hard and soft
738 sweeps from unphased genotypes by multilocus genotype identity. *Genetics* 210:1429-
739 1452.

- 740 Hewavitharane H, Warnakulasooriya H, Wajira Kumara G. 2010. Constraints to expansion
741 of cowpea and mungbean under rain-fed farming in Anuradhapura District. In.
742 Hirano H. 2021. Basic 7S globulin in plants. *Journal of Proteomics* 240:104209.
- 743 Huala E, Dickerman AW, Garcia-Hernandez M, Weems D, Reiser L, LaFond F, Hanley D,
744 Kiphart D, Zhuang M, Huang W. 2001. The Arabidopsis Information Resource (TAIR): a
745 comprehensive database and web-based information retrieval, analysis, and visualization
746 system for a model plant. *Nucleic acids research* 29:102-105.
- 747 Huang X, Kurata N, Wang Z-X, Wang A, Zhao Q, Zhao Y, Liu K, Lu H, Li W, Guo Y.
748 2012. A map of rice genome variation reveals the origin of cultivated rice. *Nature* 490:497-
749 501.
- 750 Huang X, Zhao Y, Li C, Wang A, Zhao Q, Li W, Guo Y, Deng L, Zhu C, Fan D. 2012.
751 Genome-wide association study of flowering time and grain yield traits in a worldwide
752 collection of rice germplasm. *Nature genetics* 44:32-39.
- 753 Huerta-Cepas J, Forslund K, Coelho LP, Szklarczyk D, Jensen LJ, Von Mering C, Bork P.
754 2017. Fast genome-wide functional annotation through orthology assignment by eggNOG-
755 mapper. *Molecular biology and evolution* 34:2115-2122.
- 756 Hufford MB, Xu X, Van Heerwaarden J, Pyhäjärvi T, Chia J-M, Cartwright RA, Elshire
757 RJ, Glaubitz JC, Guill KE, Kaeppler SM. 2012. Comparative population genomics of
758 maize domestication and improvement. *Nature genetics* 44:808-811.
- 759 Huson DH, Bryant D. 2006. Application of phylogenetic networks in evolutionary studies.
760 *Molecular biology and evolution* 23:254-267.
- 761 Huyghe C. 1998. Genetics and genetic modifications of plant architecture in grain legumes:
762 a review. *Agronomie* 18:383-411.
- 763 Isemura T, Kaga A, Tabata S, Somta P, Srinives P, Shimizu T, Jo U, Vaughan DA,
764 Tomooka N. 2012. Construction of a genetic linkage map and genetic analysis of
765 domestication related traits in mungbean (*Vigna radiata*).
- 766 Janczarek M, Rachwał K, Marzec A, Grządziel J, Palusińska-Szys M. 2015. Signal
767 molecules and cell-surface components involved in early stages of the legume–rhizobium
768 interactions. *Applied Soil Ecology* 85:94-113.
- 769 Kaga A, Shimizu T, Watanabe S, Tsubokura Y, Katayose Y, Harada K, Vaughan DA,
770 Tomooka N. 2012. Evaluation of soybean germplasm conserved in NIAS genebank and
771 development of mini core collections. *Breeding science* 61:566-592.
- 772 Kang YJ, Kim SK, Kim MY, Lestari P, Kim KH, Ha BK, Jun TH, Hwang WJ, Lee T, Lee
773 J, et al. 2014. Genome sequence of mungbean and insights into evolution within *Vigna*
774 species. *Nat Commun* 5:5443.
- 775 Kato S, Fujii K, Yumoto S, Ishimoto M, Shiraiwa T, Sayama T, Kikuchi A, Nishio T. 2015.
776 Seed yield and its components of indeterminate and determinate lines in recombinant
777 inbred lines of soybean. *Breeding science* 65:154-160.

- 778 Kato S, Sayama T, Taguchi-Shiobara F, Kikuchi A, Ishimoto M, Cober E. 2019. Effect of
779 change from a determinate to a semi-determinate growth habit on the yield and lodging
780 resistance of soybeans in the northeast region of Japan. *Breeding science* 69:151-159.
- 781 Kilgore-Norquest L, Sneller C. 2000. Effect of stem termination on soybean traits in
782 southern US production systems. *Crop Science* 40:83-90.
- 783 Kim D, Langmead B, Salzberg SL. 2015. HISAT: a fast spliced aligner with low memory
784 requirements. *Nature methods* 12:357-360.
- 785 Kim M-S, Lozano R, Kim JH, Bae DN, Kim S-T, Park J-H, Choi MS, Kim J, Ok H-C,
786 Park S-K. 2021. The patterns of deleterious mutations during the domestication of soybean.
787 *Nature communications* 12:1-14.
- 788 Kumar R, Sharma V, Suresh S, Ramrao DP, Veershetty A, Kumar S, Priscilla K, Hangargi
789 B, Narasanna R, Pandey MK. 2021. Understanding Omics Driven Plant Improvement and
790 de novo Crop Domestication: Some Examples. *Frontiers in genetics*:415.
- 791 Lawn R. 1989. Agronomic and physiological constraints to the productivity of tropical
792 grain legumes and prospects for improvement. *Experimental Agriculture* 25:509-528.
- 793 Lawn R, Rebetzke G. 2006. Variation among Australian accessions of the wild mungbean
794 (*Vigna radiata* ssp. *sublobata*) for traits of agronomic, adaptive, or taxonomic interest.
795 *Australian Journal of Agricultural Research* 57:119-132.
- 796 Lawn RJ, Cottrell A, Pastures CLSLQ editors.; 1988.
- 797 Leigh JW, Bryant D. 2015. popart: full-feature software for haplotype network construction.
798 *Methods in Ecology and Evolution* 6:1110-1116.
- 799 Li C, Zhou A, Sang T. 2006. Rice domestication by reducing shattering. *science* 311:1936-
800 1939.
- 801 Li H, Durbin R. 2009. Fast and accurate short read alignment with Burrows-Wheeler
802 transform. *Bioinformatics* 25:1754-1760.
- 803 Li S. 2016. The Ben Cao Gang Mu. In. *The Ben Cao Gang Mu*: University of California
804 Press.
- 805 Li S, Ding Y, Zhang D, Wang X, Tang X, Dai D, Jin H, Lee SH, Cai C, Ma J. 2018. Parallel
806 domestication with a broad mutational spectrum of determinate stem growth habit in
807 leguminous crops. *The Plant Journal* 96:761-771.
- 808 Li S-W, Shi R-F, Leng Y. 2015. De novo characterization of the mung bean transcriptome
809 and transcriptomic analysis of adventitious rooting in seedlings using RNA-Seq. *PloS one*
810 10:e0132969.
- 811 Li Y-h, Zhao S-c, Ma J-x, Li D, Yan L, Li J, Qi X-t, Guo X-s, Zhang L, He W-m. 2013.
812 Molecular footprints of domestication and improvement in soybean revealed by whole
813 genome re-sequencing. *BMC genomics* 14:1-12.
- 814 Liu G, Zhao L, Averitt BJ, Liu Y, Zhang B, Chang R, Ma Y, Luan X, Guan R, Qiu L. 2015.
815 Geographical distribution of GmTfl1 alleles in Chinese soybean varieties. *The Crop*
816 *Journal* 3:371-378.

- 817 Liu H, Li Q, Xing Y. 2018. Genes contributing to domestication of rice seed traits and its
818 global expansion. *Genes* 9:489.
- 819 Liu MS, Kuo TC, Ko CY, Wu DC, Li KY, Lin WJ, Lin CP, Wang YW, Schafleitner R, Lo
820 HF, et al. 2016. Genomic and transcriptomic comparison of nucleotide variations for
821 insights into bruchid resistance of mungbean (*Vigna radiata* [L.] R. Wilczek). *BMC Plant*
822 *Biol* 16:46.
- 823 Livak KJ, Schmittgen TD. 2001. Analysis of relative gene expression data using real-time
824 quantitative PCR and the $2^{-\Delta\Delta CT}$ method. *methods* 25:402-408.
- 825 Mangini G, Blanco A, Nigro D, Signorile MA, Simeone R. 2021. Candidate genes and
826 quantitative trait loci for grain yield and seed size in durum wheat. *Plants* 10:312.
- 827 Marcott SA, Shakun JD, Clark PU, Mix AC. 2013. A reconstruction of regional and global
828 temperature for the past 11,300 years. *science* 339:1198-1201.
- 829 Martin M. 2011. Cutadapt removes adapter sequences from high-throughput sequencing
830 reads. *EMBnet. journal* 17:10-12.
- 831 McKenna A, Hanna M, Banks E, Sivachenko A, Cibulskis K, Kernytzky A, Garimella K,
832 Altshuler D, Gabriel S, Daly M. 2010. The Genome Analysis Toolkit: a MapReduce
833 framework for analyzing next-generation DNA sequencing data. *Genome research*
834 20:1297-1303.
- 835 Mendoza EMT, Adachi M, Bernardo AEN, Utsumi S. 2001. Mungbean [*Vigna radiata* (L.)
836 Wilczek] globulins: purification and characterization. *Journal of Agricultural and Food*
837 *Chemistry* 49:1552-1558.
- 838 Meyer RS, Purugganan MD. 2013. Evolution of crop species: genetics of domestication
839 and diversification. *Nature reviews genetics* 14:840-852.
- 840 Nair RM, Schafleitner R, Lee S-H. 2020. *The mungbean genome*: Springer.
- 841 Nguyen TD, Lawn R, Bielig L. 2012. Expression and inheritance of perenniality and other
842 qualitative traits in hybrids between mungbean cultivars and Australian wild accessions.
843 *Crop and Pasture Science* 63:619-634.
- 844 Noble TJ, Tao Y, Mace ES, Williams B, Jordan DR, Douglas CA, Mundree SG. 2018.
845 Characterization of linkage disequilibrium and population structure in a mungbean
846 diversity panel. *Frontiers in plant science* 8:2102.
- 847 Norihiko T, Kaga A, Isemura T, Vaughan D, Srinives P, Somta P, Thadavong S,
848 Bounphanousay C, Kanyavong K, Inthapanya P editors. *Proceeding of the 14th NIAS*
849 *international workshop on Genetic Resources, Genetic and Comparative Genomics of*
850 *Legumes (Glycine and Vigna)*. 2010.
- 851 Paradis E, Schliep K. 2018. ape 5.0: an environment for modern phylogenetics and
852 evolutionary analyses in R. *Bioinformatics* 35:526-528.
- 853 Parker TA, Lo S, Gepts P. 2021. Pod shattering in grain legumes: emerging genetic and
854 environment-related patterns. *The Plant Cell* 33:179-199.

- 855 Pavlidis P, Živković D, Stamatakis A, Alachiotis N. 2013. SweeD: likelihood-based
856 detection of selective sweeps in thousands of genomes. *Molecular biology and evolution*
857 30:2224-2234.
- 858 Perteua M, Perteua GM, Antonescu CM, Chang T-C, Mendell JT, Salzberg SL. 2015.
859 StringTie enables improved reconstruction of a transcriptome from RNA-seq reads. *Nature*
860 *biotechnology* 33:290-295.
- 861 Pham A-T, Shannon JG, Bilyeu KD. 2012. Combinations of mutant FAD2 and FAD3
862 genes to produce high oleic acid and low linolenic acid soybean oil. *Theoretical and*
863 *Applied Genetics* 125:503-515.
- 864 Phillips SJ, Anderson RP, Schapire RE. 2006. Maximum entropy modeling of species
865 geographic distributions. *Ecological Modelling* 190:231-259.
- 866 Pierce BA. 2012. *Genetics: A Conceptual Approach*. W. H. Freeman.
- 867 Pomar F, Merino F, Barceló AR. 2002. O-4-Linked coniferyl and sinapyl aldehydes in
868 lignifying cell walls are the main targets of the Wiesner (phloroglucinol-HCl) reaction.
869 *Protoplasma* 220:0017-0028.
- 870 Purcell S, Neale B, Todd-Brown K, Thomas L, Ferreira MA, Bender D, Maller J, Sklar P,
871 De Bakker PI, Daly MJ. 2007. PLINK: a tool set for whole-genome association and
872 population-based linkage analyses. *The American journal of human genetics* 81:559-575.
- 873 Purugganan MD, Fuller DQ. 2009. The nature of selection during plant domestication.
874 *Nature* 457:843-848.
- 875 Roucou A, Violle C, Fort F, Roumet P, Ecarnot M, Vile D. 2018. Shifts in plant functional
876 strategies over the course of wheat domestication. *Journal of Applied Ecology* 55:25-37.
- 877 Sakai H, Naito K, Takahashi Y, Sato T, Yamamoto T, Muto I, Itoh T, Tomooka N. 2016.
878 The Vigna Genome Server, 'Vig GS': A genomic knowledge base of the genus *Vigna* based
879 on high-quality, annotated genome sequence of the Azuki Bean, *Vigna angularis* (Willd.)
880 Ohwi & Ohashi. *Plant and Cell Physiology* 57:e2-e2.
- 881 Schouten HJ, Tikunov Y, Verkerke W, Finkers R, Bovy A, Bai Y, Visser RG. 2019.
882 Breeding has increased the diversity of cultivated tomato in The Netherlands. *Frontiers in*
883 *plant science*:1606.
- 884 Slater GSC, Birney E. 2005. Automated generation of heuristics for biological sequence
885 comparison. *BMC bioinformatics* 6:1-11.
- 886 Song Y, Sun E-tZ, Sun S-C. 1997. *Chinese technology in the seventeenth century*: Courier
887 Corporation.
- 888 Specht JE, Diers BW, Nelson RL, de Toledo JFF, Torrión JA, Grassini P. 2014. Soybean.
889 *Yield gains in major US field crops* 33:311-355.
- 890 Stanke M, Keller O, Gunduz I, Hayes A, Waack S, Morgenstern B. 2006. AUGUSTUS:
891 ab initio prediction of alternative transcripts. *Nucleic acids research* 34:W435-W439.
- 892 Takahashi Y, Kongjaimun A, Muto C, Kobayashi Y, Kumagai M, Sakai H, Satou K,
893 Teruya K, Shiroma A, Shimoji M. 2020. Same locus for non-shattering seed pod in two

894 independently domesticated legumes, *Vigna angularis* and *Vigna unguiculata*. *Frontiers in*
895 *genetics* 11:748.

896 Tamura K, Stecher G, Kumar S. 2021. MEGA11: molecular evolutionary genetics analysis
897 version 11. *Molecular biology and evolution* 38:3022-3027.

898 Tateishi Y. 1996. Systematics of the species of *Vigna* subgenus *Ceratotropis*. *Mungbean*
899 *Germplasm: collection and utilization for breeding program.*:9-24.

900 Terhorst J, Kamm JA, Song YS. 2017. Robust and scalable inference of population history
901 from hundreds of unphased whole genomes. *Nat Genet* 49:303-309.

902 Tobler R, Rohrlach A, Soubrier J, Bover P, Llamas B, Tuke J, Bean N, Abdullah-Highfold
903 A, Agius S, O'Donoghue A. 2017. Aboriginal mitogenomes reveal 50,000 years of
904 regionalism in Australia. *Nature* 544:180-184.

905 Van Bel M, Diels T, Vancaester E, Kreft L, Botzki A, Van de Peer Y, Coppens F,
906 Vandepoele K. 2018. PLAZA 4.0: an integrative resource for functional, evolutionary and
907 comparative plant genomics. *Nucleic acids research* 46:D1190-D1196.

908 Van der Auwera GA, Carneiro MO, Hartl C, Poplin R, Del Angel G, Levy-Moonshine A,
909 Jordan T, Shakir K, Roazen D, Thibault J. 2013. From FastQ data to high-confidence
910 variant calls: the genome analysis toolkit best practices pipeline. *Current protocols in*
911 *bioinformatics* 43:11.10. 11-11.10. 33.

912 Vavilov NI. 1922. The law of homologous series in variation. *Journal of genetics* 12:47-
913 89.

914 Vavilov NI. 1951. The origin, variation, immunity and breeding of cultivated plants: LWW.
915 von Wettberg EJB, Chang PL, Basdemir F, Carrasquilla-Garcia N, Korbu LB, Moenga SM,
916 Bedada G, Greenlon A, Moriuchi KS, Singh V, et al. 2018. Ecology and genomics of an
917 important crop wild relative as a prelude to agricultural innovation. *Nat Commun* 9:649.

918 Wang L, Stegemann JP. 2010. Extraction of high quality RNA from polysaccharide
919 matrices using cetyltrimethylammonium bromide. *Biomaterials* 31:1612-1618.

920 Xia Z, Watanabe S, Yamada T, Tsubokura Y, Nakashima H, Zhai H, Anai T, Sato S,
921 Yamazaki T, Lü S. 2012. Positional cloning and characterization reveal the molecular basis
922 for soybean maturity locus E1 that regulates photoperiodic flowering. *Proceedings of the*
923 *National Academy of Sciences* 109:E2155-E2164.

924 Xie M, Zhang J, Tschaplinski TJ, Tuskan GA, Chen J-G, Muchero W. 2018. Regulation of
925 lignin biosynthesis and its role in growth-defense tradeoffs. *Frontiers in plant science*:1427.

926 Yang Z. 2007. PAML 4: phylogenetic analysis by maximum likelihood. *Molecular biology*
927 *and evolution* 24:1586-1591.

928 Yang Z, Nielsen R. 2000. Estimating synonymous and nonsynonymous substitution rates
929 under realistic evolutionary models. *Molecular biology and evolution* 17:32-43.

930 Zhang C, Dong S-S, Xu J-Y, He W-M, Yang T-L. 2019. PopLDdecay: a fast and effective
931 tool for linkage disequilibrium decay analysis based on variant call format files.
932 *Bioinformatics* 35:1786-1788.

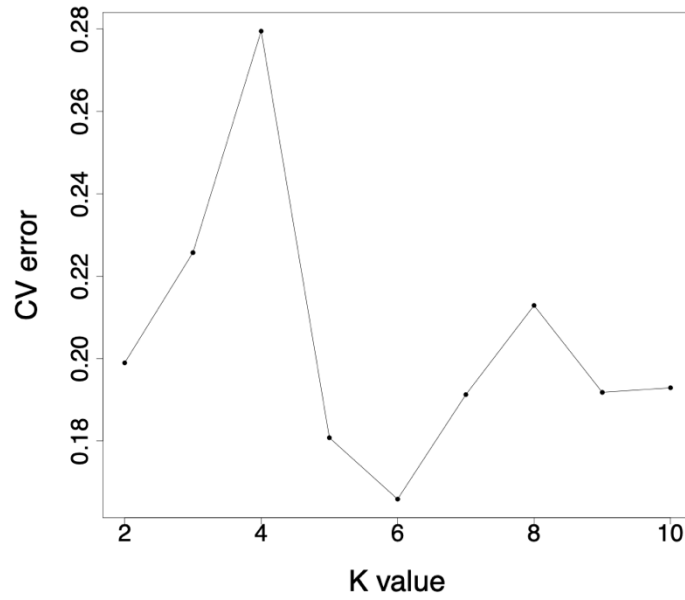
933 Zhang J, Song Q, Cregan PB, Nelson RL, Wang X, Wu J, Jiang G-L. 2015. Genome-wide
934 association study for flowering time, maturity dates and plant height in early maturing
935 soybean (*Glycine max*) germplasm. *BMC genomics* 16:1-11.
936 Zhou Z, Jiang Y, Wang Z, Gou Z, Lyu J, Li W, Yu Y, Shu L, Zhao Y, Ma Y. 2015.
937 Resequencing 302 wild and cultivated accessions identifies genes related to domestication
938 and improvement in soybean. *Nature biotechnology* 33:408-414.

939

940

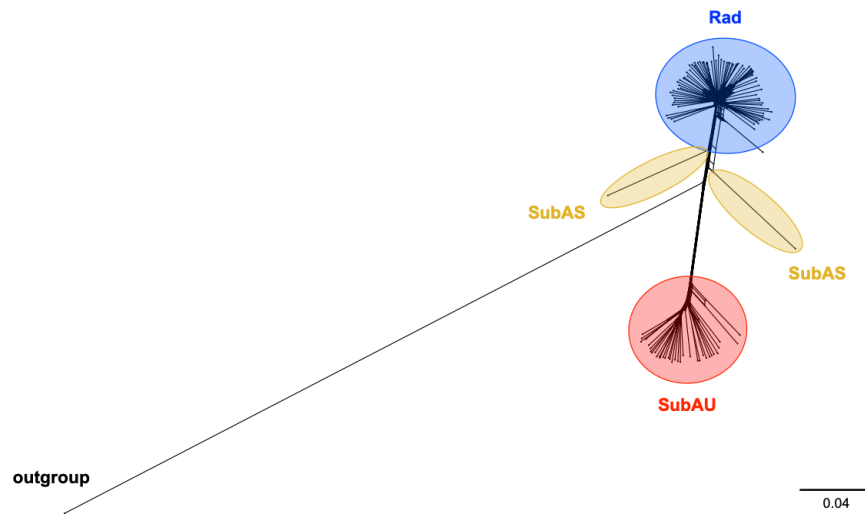
941 **Supplementary figures**

942



943 **Supplementary Fig. S1. Cross-validation error of each K value.**

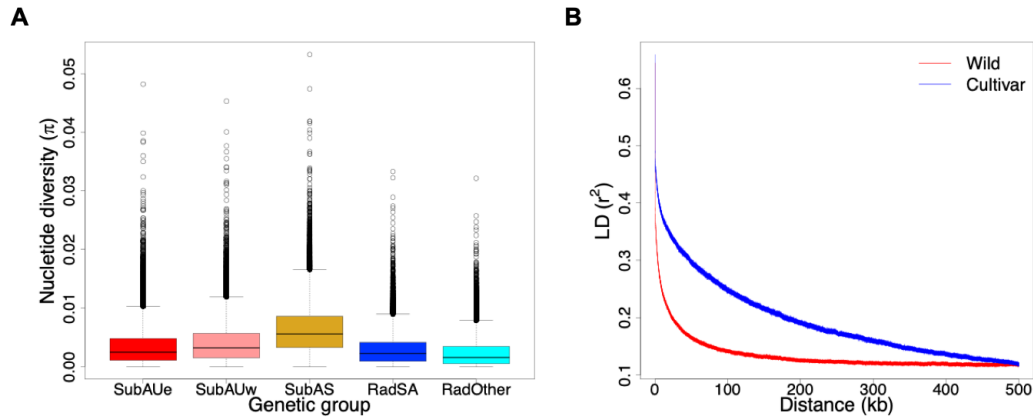
944



945

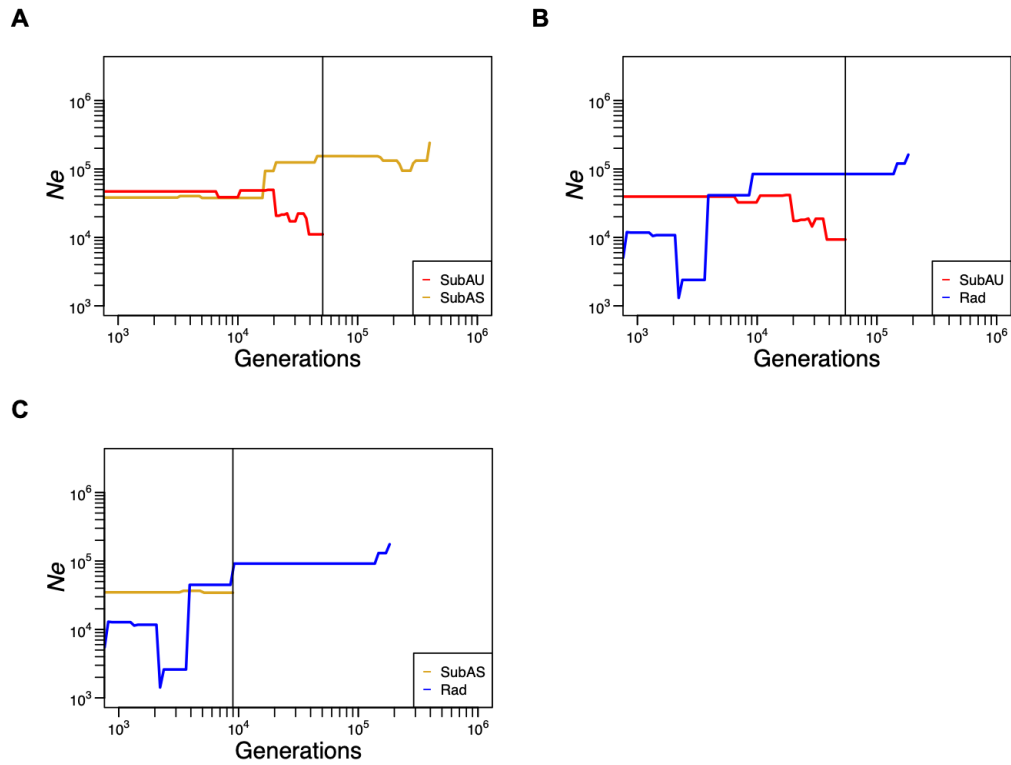
946 **Supplementary Fig. S2. Phylogenetic network of the 114 mungbean accessions and**
947 **one outgroup.**

948



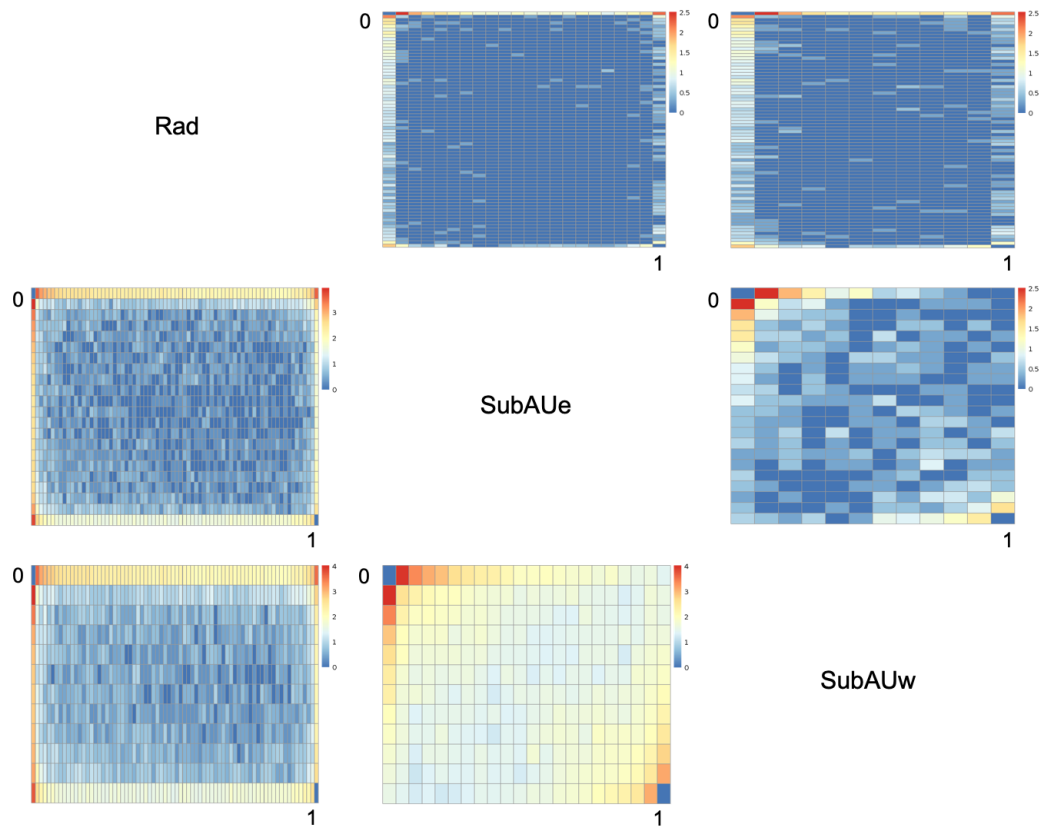
949 **Supplementary Fig. S3. Genetic diversity of mungbean.** (A) Nucleotide diversity (π) in
950 the 10kb window of the three wild genetic groups (SubAUe, SubAUw, and SubAS) and
951 the two cultivated genetic groups (RadSA and RadOther). The boxes indicate medians and
952 interquartile ranges, whiskers indicate 95% values, and additional points in each boxplot
953 represent outliers. (B) Decay of linkage disequilibrium (LD) of wild and cultivated
954 populations.

955



956 **Supplementary Fig. S4. Pairwise population divergence time.** (A) SubAU and SubAS
957 (B) SubAU and Rad (C) SubAS and Rad. The vertical black lines denote the estimated
958 divergence time.

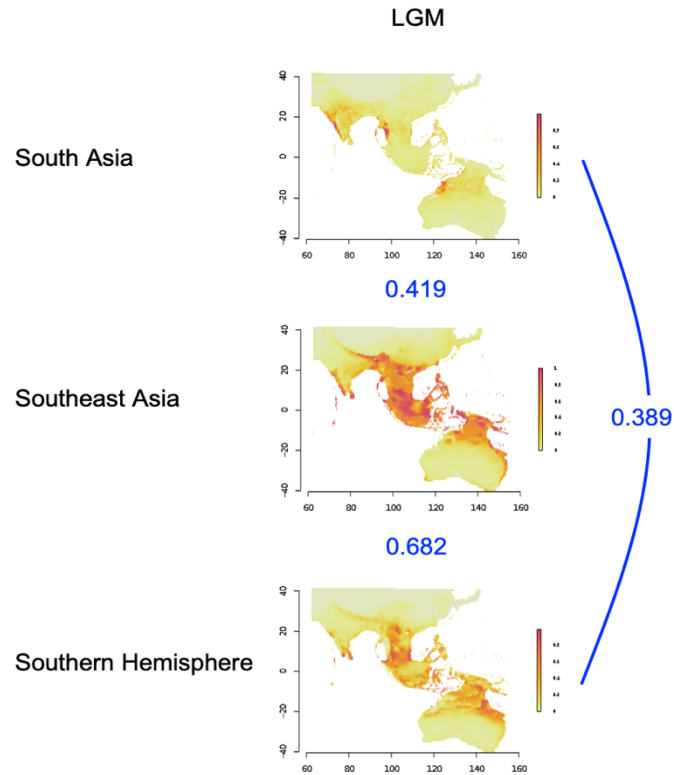
959



960

961 **Supplementary Fig. S5. Two-dimensional site frequency spectrum (2D SFS) between**
962 **Rad, SubAUe, and SubAUw groups.** The upper triangle plots are 2D SFS of the SNPs
963 with high impact estimated by SnpEff; the lower triangle plots are the 2D SFS of the 4-fold
964 degenerate SNPs. Colors reflect the log₁₀ number of SNPs.

965

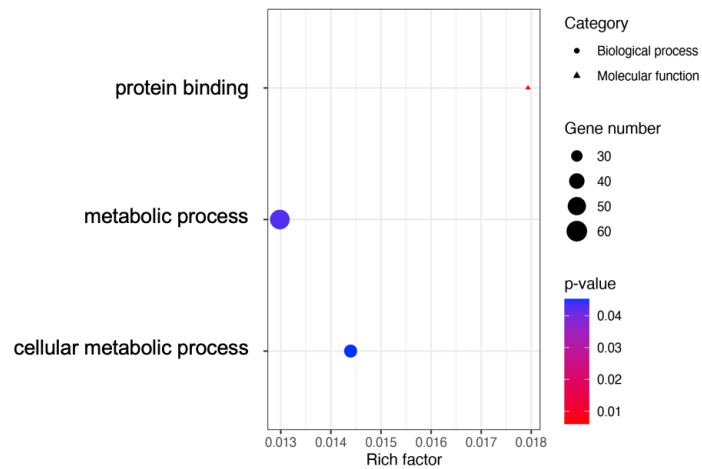


966

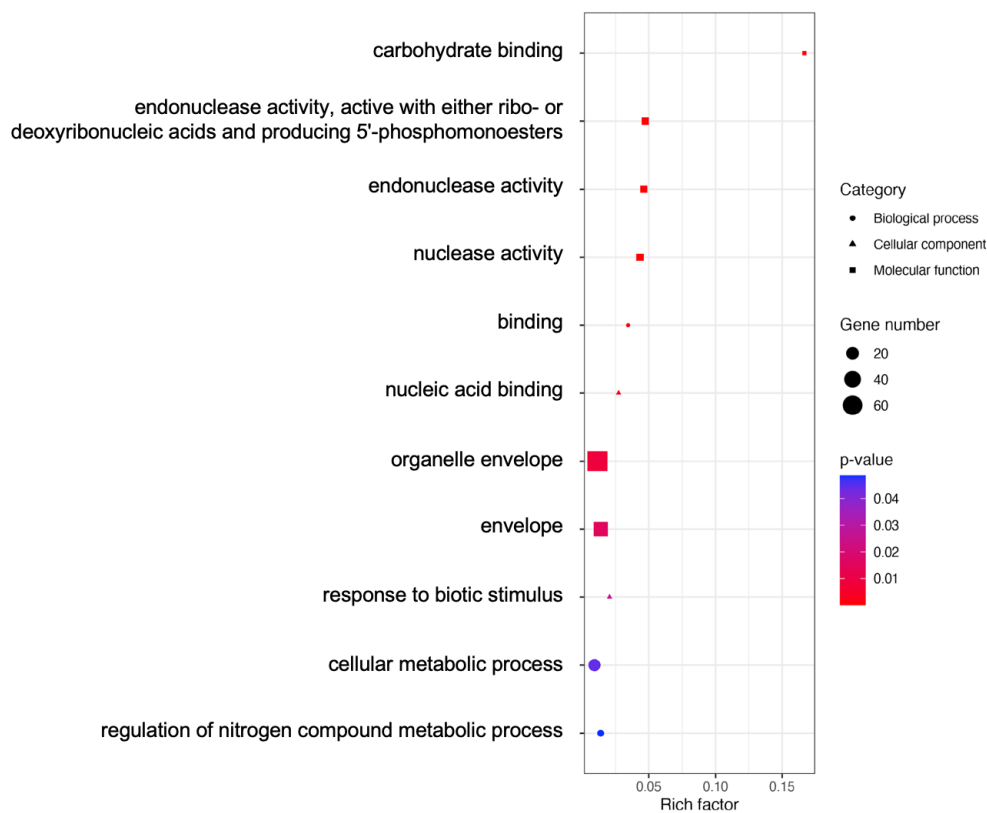
967 **Supplementary Fig. S6. Ecological niche modeling of suitable habitats for the wild**
968 **mungbean populations in South Asia, Southeast Asia, and South Hemisphere in Last**
969 **Glacial Maximum (22 kya).** Colors represent niche suitability. The three graphs (South
970 Asia, Southeast Asia, and Southern Hemisphere) represent niche models constructed from
971 the presence data of wild mungbean from these regions and projected to the whole
972 geographical extent. Data of the Last Glacial Maximum (22 kya, LGM) was based on the
973 circulation model of CCSM4. The numbers in blue between pairs of modeled distribution
974 indicate the Schoner'D values, where higher values represent higher niche similarity.

975

A



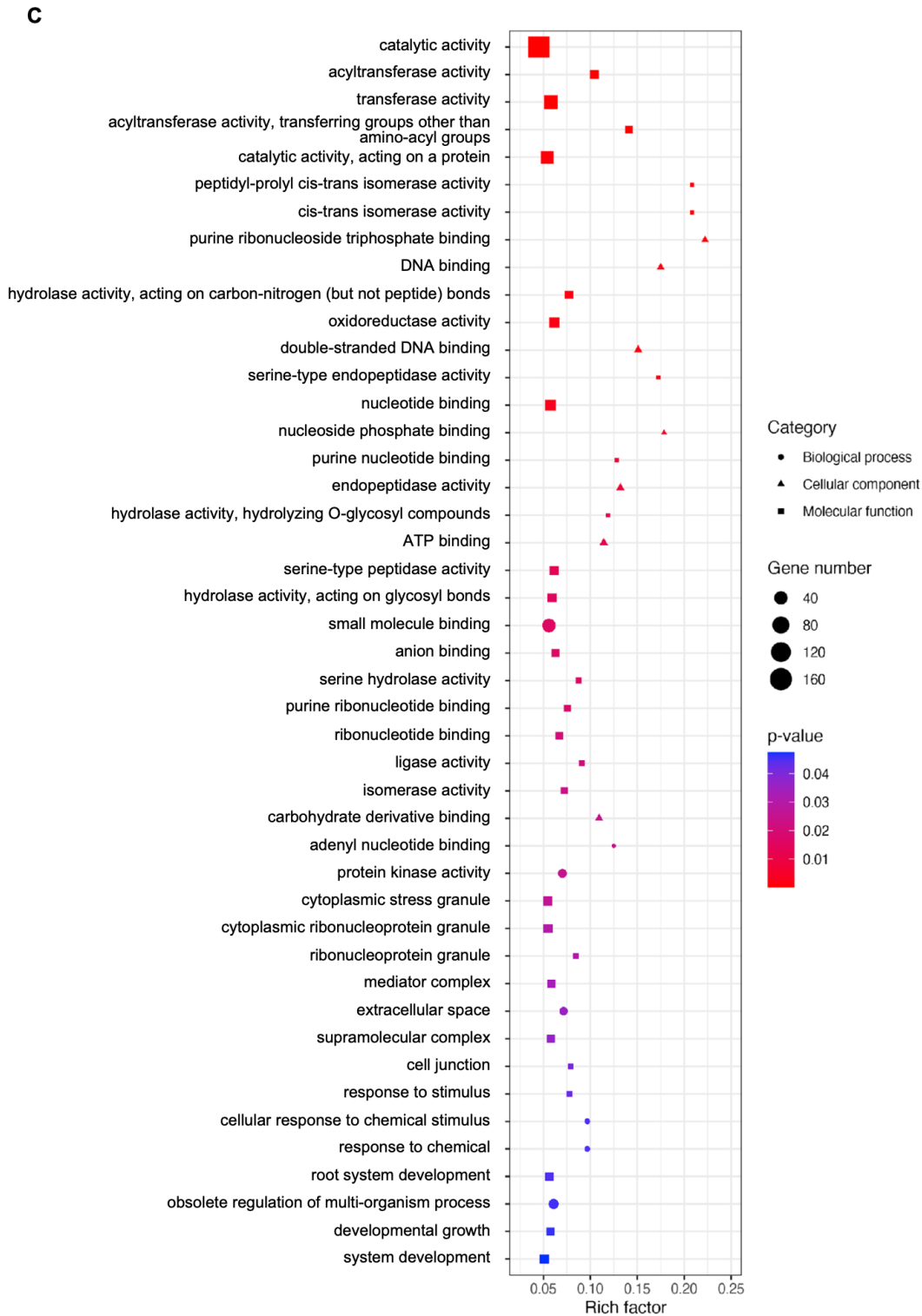
B



976

977 **Supplementary Fig. S7. Gene Ontology (GO) enrichment of candidate genes in the**
 978 **regions of signatures of selection.** Shown are the GO enrichment of candidate selective
 979 sweep genes from the (A) composite likelihood ratio (CLR) of the wild group, (B) CLR of
 980 the cultivars, and (C) reduction of diversity.

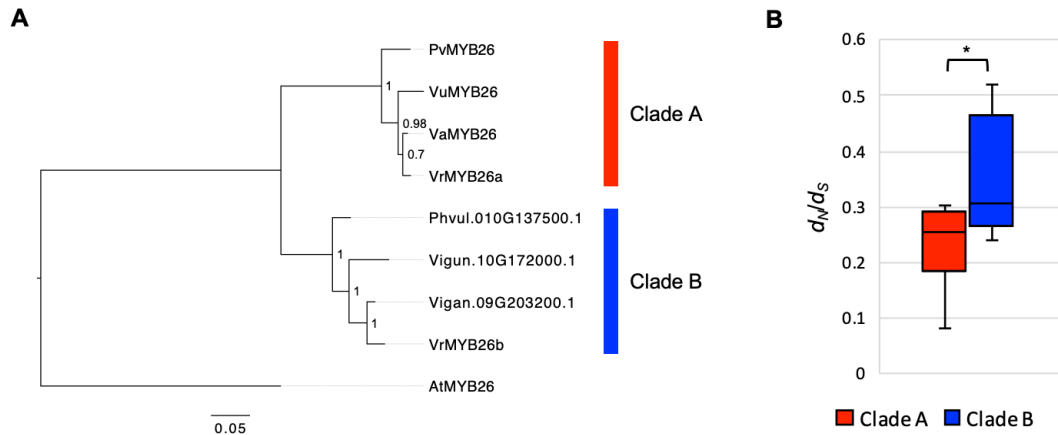
981



982

983 **Supplementary Fig. S7 (Continue).**

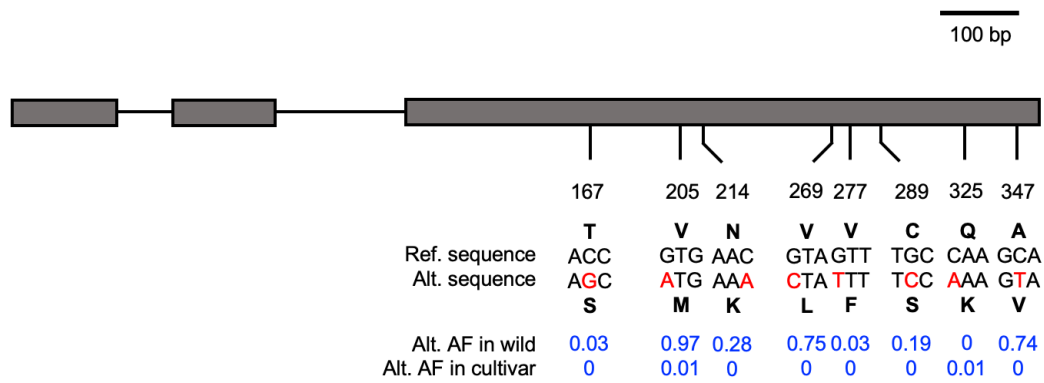
984



985

986 **Supplementary Fig. S8. Evolution of *MYB26* homologs in legumes.** (A) Maximum-
987 likelihood (ML) tree constructed from the coding sequences of the *MYB26* homologs using
988 *AtMYB26* as an outgroup. The numbers adjacent to nodes indicate the proportion of support
989 in 1,000 bootstrap re-samplings. (B) The d_N/d_S ratios of the *MYB26* orthologs are estimated
990 based on the pairwise comparison in each of the two clades in the ML tree. The boxes
991 indicate medians and interquartile ranges; the whiskers indicate 95% values (* indicates p
992 value < 0.05).

993



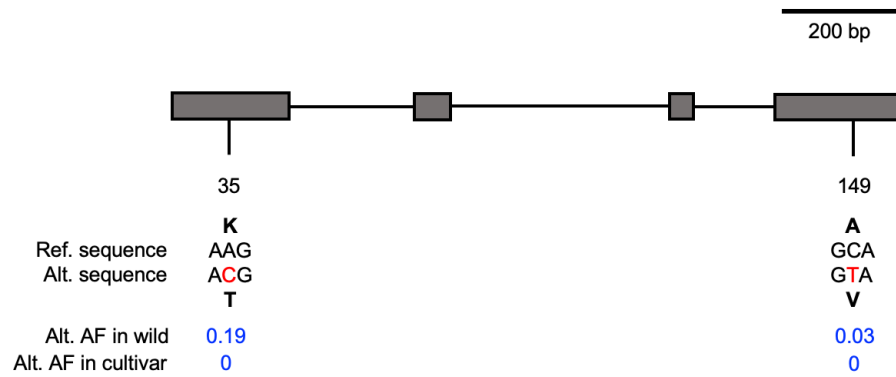
994

995 **Supplementary Fig. S9. Diagram of the *VrMYB26a* non-synonymous changes.** Shown

996 are the positions of non-synonymous SNPs and the frequency of alternative alleles (Alt.

997 AF) in wild and cultivated populations.

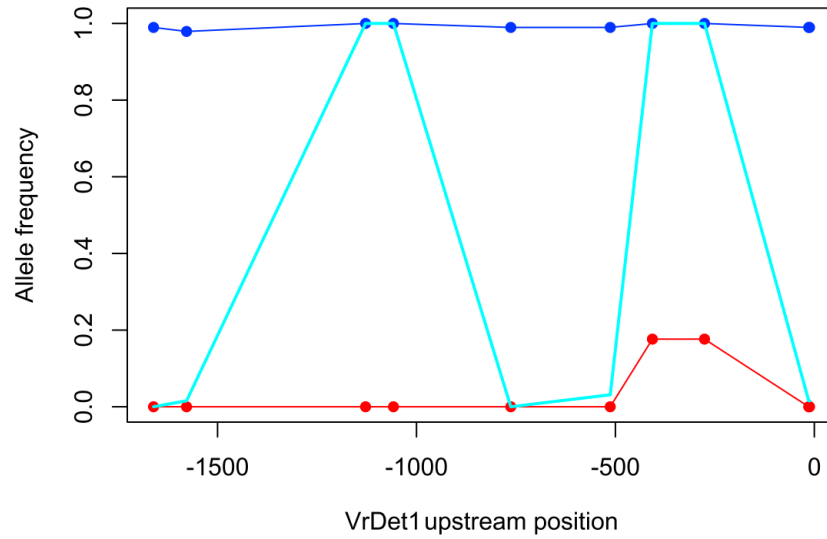
998



999

1000 **Supplementary Fig. S10. Diagram of the *VrDet1* non-synonymous changes.** Shown are
1001 the positions of non-synonymous SNPs and the frequency of alternative alleles (Alt. AF)
1002 in wild and cultivated populations.

1003



1004

1005 **Supplementary Fig. S11. Distribution of allele frequency in *VrDet1* upstream 2kb**
1006 **region among three clades (red: Clade I, sky-blue: Clade II, blue: Clade III).** Nine
1007 diagnostic SNPs with the large allele frequency differences between Clade I and III were
1008 shown, and the major allele in Clade III was used to estimate allele frequency.

Supplementary tables

Supplementary Table S1. Summary of sequencing data for each accession analyzed in this study

| Accession | Average base quality | Total reads | Total bases | Mapping reads | Read mapping rate (%) | Sequencing depth (X) |
|------------------|-----------------------------|--------------------|--------------------|----------------------|------------------------------|-----------------------------|
| Crystal | 38.6 | 196483180 | 28727374463 | 195351734 | 99.42 | 62.03 |
| NAM1 | 39 | 127533934 | 19010063503 | 119996800 | 94.09 | 41.05 |
| NAM2 | 39 | 126703124 | 18890287992 | 122616672 | 96.77 | 40.79 |
| NAM3 | 38.7 | 148349752 | 22112564826 | 144734909 | 97.56 | 47.75 |
| NAM4 | 38.5 | 94156396 | 14016993080 | 93171459 | 98.95 | 30.27 |
| NAM5 | 38.8 | 119703610 | 17821660108 | 116774122 | 97.55 | 38.48 |
| NAM6 | 39 | 124431120 | 18546889117 | 122036022 | 98.08 | 40.05 |
| NAM7 | 39.1 | 146988240 | 21900082222 | 146066498 | 99.37 | 47.29 |
| NAM8 | 39 | 114165632 | 17000285477 | 111296904 | 97.49 | 36.71 |
| NAM9 | 38.3 | 114995514 | 17175168161 | 111740019 | 97.17 | 37.09 |
| NAM10 | 38.7 | 147767224 | 22062903874 | 144915289 | 98.07 | 47.64 |
| NAM11 | 38.5 | 129858206 | 19387275676 | 124465045 | 95.85 | 41.87 |
| NAM12 | 38.4 | 162972618 | 24344134422 | 156681072 | 96.14 | 52.57 |

| | | | | | | |
|------------|------|-----------|-------------|-----------|-------|-------|
| NAM13 | 38.6 | 142539446 | 21285763164 | 136730232 | 95.92 | 45.97 |
| NAM15 | 38.5 | 134863986 | 20121555751 | 131533360 | 97.53 | 43.45 |
| NAM16 | 38.7 | 85364434 | 12748587321 | 84299239 | 98.75 | 27.53 |
| NAM17 | 38.1 | 134722504 | 20147479994 | 133167359 | 98.85 | 43.51 |
| NAM18 | 38.7 | 141671450 | 21158317508 | 140643256 | 99.27 | 45.69 |
| NAM19 | 38.4 | 112779164 | 16813978606 | 111409295 | 98.79 | 36.31 |
| NAM20 | 38.5 | 130499886 | 19490475112 | 129397877 | 99.16 | 42.09 |
| NAM21 | 38.6 | 132985114 | 19856334359 | 131512282 | 98.89 | 42.88 |
| NAM22 | 38.4 | 107398574 | 16050627709 | 105897481 | 98.60 | 34.66 |
| NAM23 | 38.9 | 143669612 | 21454673884 | 142409613 | 99.12 | 46.33 |
| NAM24 | 38.3 | 131334734 | 19410296478 | 129409725 | 98.53 | 41.92 |
| NAM26 | 38.1 | 114831936 | 16962317946 | 113213499 | 98.59 | 36.63 |
| NAM27 | 38.1 | 126707904 | 18693602904 | 125423094 | 98.99 | 40.37 |
| VI000020AY | 38.3 | 107685230 | 15714113847 | 107149544 | 99.50 | 33.93 |
| VI000099AG | 37.9 | 123351108 | 18172014038 | 121695136 | 98.66 | 39.24 |
| VI000232AG | 37.9 | 115094024 | 16952613959 | 114295135 | 99.31 | 36.61 |
| VI000238AG | 38 | 117628680 | 17337135019 | 116884614 | 99.37 | 37.44 |

| | | | | | | |
|--------------|------|-----------|-------------|-----------|-------|-------|
| VI000542BY | 37.9 | 114540288 | 16892176117 | 113376374 | 98.98 | 36.48 |
| VI000578AG | 37.9 | 140304700 | 20699908970 | 139324816 | 99.30 | 44.70 |
| VI000625B-BR | 38 | 110947438 | 16362038748 | 110341377 | 99.45 | 35.33 |
| VI000938AG | 38.1 | 113916038 | 16771866336 | 113054013 | 99.24 | 36.22 |
| VI001191BG | 39 | 91140902 | 13357067934 | 90567830 | 99.37 | 28.84 |
| VI001435AG | 38 | 117448760 | 17467476874 | 115727581 | 98.53 | 37.72 |
| VI001509AG | 38.2 | 108920614 | 16166073569 | 108153675 | 99.30 | 34.91 |
| VI001514AG | 38.6 | 97989586 | 14525965237 | 95722966 | 97.69 | 31.37 |
| VI001728AG | 38.7 | 99679194 | 14672353144 | 99014305 | 99.33 | 31.68 |
| VI001806BG | 38.5 | 107456990 | 15849661425 | 106402936 | 99.02 | 34.23 |
| VI002176BG | 38.6 | 103202330 | 15192308217 | 102428510 | 99.25 | 32.81 |
| VI002197BG | 38.3 | 106389320 | 15792270028 | 105625140 | 99.28 | 34.10 |
| VI002239AG | 38.7 | 100855684 | 14857800232 | 100096208 | 99.25 | 32.08 |
| VI002456AG | 38.8 | 105440890 | 15528929567 | 104898680 | 99.49 | 33.53 |
| VI002647AG | 38.7 | 116052796 | 17101843320 | 114535313 | 98.69 | 36.93 |
| VI002859BG | 38.6 | 99282868 | 14624346753 | 98349936 | 99.06 | 31.58 |
| VI002872BG | 38.5 | 95386498 | 14051534759 | 94675667 | 99.25 | 30.34 |

| | | | | | | |
|---------------|------|-----------|-------------|-----------|-------|-------|
| VI002934AG | 38.6 | 100956428 | 14842385806 | 100172814 | 99.22 | 32.05 |
| VI002986AG | 38.1 | 110264536 | 16338853680 | 109309431 | 99.13 | 35.28 |
| VI003057BG | 38.7 | 105522924 | 15542296441 | 104814382 | 99.33 | 33.56 |
| VI003135B-BL | 38.5 | 94387268 | 14047038329 | 93390608 | 98.94 | 30.33 |
| VI003255AG | 37.8 | 99055188 | 14755125143 | 97726020 | 98.66 | 31.86 |
| VI003337BG | 38.7 | 89894206 | 13255609595 | 89094914 | 99.11 | 28.62 |
| VI003456AG | 38.8 | 106278456 | 15679639468 | 105088651 | 98.88 | 33.86 |
| VI003465BG | 38.4 | 115632864 | 16997323784 | 114587126 | 99.10 | 36.70 |
| VI003480BG | 38.2 | 100627792 | 14956434651 | 99782886 | 99.16 | 32.30 |
| VI003534BG | 38.3 | 108905074 | 16172568035 | 106698088 | 97.97 | 34.92 |
| VI003699B-BR | 38.7 | 103393636 | 15254347310 | 102441163 | 99.08 | 32.94 |
| VI003894B-BLM | 38.2 | 94378774 | 14002556256 | 93400898 | 98.96 | 30.24 |
| VI003925B-BLM | 38.7 | 98579442 | 14534665858 | 97866584 | 99.28 | 31.39 |
| VI003948B-BR | 38.8 | 110602470 | 16320394085 | 109674951 | 99.16 | 35.24 |
| VI004069BG | 38.2 | 108221038 | 16097887913 | 106939499 | 98.82 | 34.76 |
| VI004184AG | 38.1 | 111065672 | 16500464023 | 110042604 | 99.08 | 35.63 |
| VI004243B-BR | 38.3 | 97858906 | 14538755397 | 97146535 | 99.27 | 31.40 |

| | | | | | | |
|---------------|------|-----------|-------------|-----------|-------|-------|
| VI004244B-BR | 38.3 | 117199772 | 17404677979 | 116163988 | 99.12 | 37.58 |
| VI004312AG | 38.7 | 94910852 | 14001885094 | 94193537 | 99.24 | 30.24 |
| VI004432B-BR | 38.7 | 94641712 | 13970450807 | 93998848 | 99.32 | 30.17 |
| VI004666AG | 38.8 | 98028200 | 14463568142 | 97255573 | 99.21 | 31.23 |
| VI004853BG | 38.6 | 115299028 | 17005975646 | 114380607 | 99.20 | 36.72 |
| VI004956AG | 37.9 | 108132250 | 16071655376 | 107196827 | 99.13 | 34.71 |
| VI004965BG | 38.1 | 109098962 | 16219658117 | 108270161 | 99.24 | 35.03 |
| VI004973B-BLM | 38.3 | 115857178 | 17193286881 | 115048196 | 99.30 | 37.13 |
| VI005022BG | 38 | 116969410 | 17418599262 | 115808887 | 99.01 | 37.61 |
| VI005030BY | 38.1 | 90933136 | 13520558513 | 88335353 | 97.14 | 29.20 |
| VI005041AG | 38.6 | 117271888 | 17308635737 | 115911704 | 98.84 | 37.38 |
| VI014178BG | 38.2 | 121729992 | 18099953464 | 120803779 | 99.24 | 39.09 |
| VI064196 | 38.5 | 102168058 | 15189855794 | 101020176 | 98.88 | 32.80 |
| VI064197 | 38.4 | 99581820 | 14825078697 | 98852502 | 99.27 | 32.01 |
| BCP_075 | 38.7 | 64824598 | 9723689700 | 63537223 | 98.01 | 21.00 |
| BCP_094 | 38.6 | 64589664 | 9688449600 | 62820738 | 97.26 | 20.92 |
| CPI_106935 | 38.7 | 61166356 | 9174953400 | 59681199 | 97.57 | 19.81 |

| | | | | | | |
|------------|------|----------|-------------|----------|-------|-------|
| CPI_107220 | 38.5 | 67033788 | 10055068200 | 65024377 | 97.00 | 21.71 |
| CQ_1971 | 40 | 71679290 | 10751893500 | 71057178 | 99.13 | 23.22 |
| CQ_2225 | 38.6 | 71861326 | 10779198900 | 70765501 | 98.48 | 23.28 |
| CQ_2226 | 38.9 | 60240702 | 9036105300 | 56521676 | 93.83 | 19.51 |
| CQ_2227 | 38.8 | 62187366 | 9328104900 | 60896815 | 97.92 | 20.14 |
| CQ_2234 | 38.3 | 72144358 | 10821653700 | 69167055 | 95.87 | 23.37 |
| CQ_2238 | 38.2 | 60553920 | 9083088000 | 56171606 | 92.76 | 19.61 |
| CQ_2244 | 38.6 | 68888586 | 10333287900 | 51527945 | 74.80 | 22.31 |
| CQ_2326 | 38.7 | 71213930 | 10682089500 | 70093515 | 98.43 | 23.07 |
| CQ_2649 | 38.3 | 55374758 | 8306213700 | 53865466 | 97.27 | 17.94 |
| CQ_2650 | 38.7 | 63250020 | 9487503000 | 61571908 | 97.35 | 20.49 |
| CQ_2651 | 38.7 | 72644490 | 10896673500 | 66170123 | 91.09 | 23.53 |
| CQ_2733 | 39.7 | 67389924 | 10108488600 | 66669731 | 98.93 | 21.83 |
| CQ_2915 | 38.5 | 59197868 | 8879680200 | 58028518 | 98.02 | 19.18 |
| CQ_2926 | 38.7 | 67832232 | 10174834800 | 67026527 | 98.81 | 21.97 |
| CQ_3066 | 38.9 | 69412548 | 10411882200 | 68031185 | 98.01 | 22.48 |
| CQ_3082 | 38.6 | 77342370 | 11601355500 | 76306064 | 98.66 | 25.05 |

| | | | | | | |
|-----------|------|-----------|-------------|-----------|-------|-------|
| CQ_3086 | 38.7 | 72397190 | 10859578500 | 70795813 | 97.79 | 23.45 |
| CQ_3114 | 38.6 | 76035000 | 11405250000 | 74647437 | 98.18 | 24.63 |
| CQ_3233 | 38.5 | 69654562 | 10448184300 | 68619068 | 98.51 | 22.56 |
| CQ_3243 | 39 | 58875304 | 8831295600 | 57996075 | 98.51 | 19.07 |
| CQ_3267 | 38.8 | 69606166 | 10440924900 | 67877694 | 97.52 | 22.55 |
| CQ_3269 | 38.6 | 63373196 | 9505979400 | 61641160 | 97.27 | 20.53 |
| CQ_3283 | 38.2 | 60634948 | 9095242200 | 55522294 | 91.57 | 19.64 |
| CQ_3293 | 38.3 | 70636224 | 10595433600 | 68981512 | 97.66 | 22.88 |
| CQ_3323 | 38.6 | 69759192 | 10463878800 | 68547136 | 98.26 | 22.60 |
| Karumbyar | 38.6 | 213776592 | 31222432351 | 211497414 | 98.93 | 67.42 |
| NAM28 | 38.2 | 192620538 | 28006223559 | 190160711 | 98.72 | 60.48 |
| NAM29 | 38.4 | 187196374 | 27210646221 | 184919246 | 98.78 | 58.76 |
| NAM30 | 38.6 | 174386998 | 25414019497 | 172453908 | 98.89 | 54.88 |
| TPI_25 | 39 | 66252234 | 9937835100 | 65532983 | 98.91 | 21.46 |
| VI032155 | 38.2 | 104377702 | 15536268464 | 103054321 | 98.73 | 33.55 |
| VI032156 | 38.3 | 108713520 | 16186446077 | 107553969 | 98.93 | 34.95 |
| VI035226 | 38.3 | 97733110 | 14546845659 | 92007079 | 94.14 | 31.41 |

Supplementary Table S2. List of accessions used in this study

| Accession | Taxonomy | Country of collection | Genetic group |
|------------------|--|------------------------------|----------------------|
| Crystal | <i>Vigna radiata</i> var. <i>radiata</i> | Unknown | Admixed_Rad |
| NAM1 | <i>Vigna radiata</i> var. <i>radiata</i> | Philippines | RadOther |
| NAM2 | <i>Vigna radiata</i> var. <i>radiata</i> | Unknown | RadOther |
| NAM3 | <i>Vigna radiata</i> var. <i>radiata</i> | Unknown | Admixed_Rad |
| NAM4 | <i>Vigna radiata</i> var. <i>radiata</i> | Unknown | Admixed_Rad |
| NAM5 | <i>Vigna radiata</i> var. <i>radiata</i> | Unknown | RadOther |
| NAM6 | <i>Vigna radiata</i> var. <i>radiata</i> | Unknown | RadOther |
| NAM7 | <i>Vigna radiata</i> var. <i>radiata</i> | Unknown | Admixed_Rad |
| NAM8 | <i>Vigna radiata</i> var. <i>radiata</i> | Unknown | Admixed_Rad |
| NAM9 | <i>Vigna radiata</i> var. <i>radiata</i> | India | RadSA |
| NAM10 | <i>Vigna radiata</i> var. <i>radiata</i> | Unknown | RadSA |
| NAM11 | <i>Vigna radiata</i> var. <i>radiata</i> | Unknown | RadOther |
| NAM12 | <i>Vigna radiata</i> var. <i>radiata</i> | Unknown | RadOther |
| NAM13 | <i>Vigna radiata</i> var. <i>radiata</i> | Unknown | RadOther |
| NAM15 | <i>Vigna radiata</i> var. <i>radiata</i> | Unknown | RadOther |
| NAM16 | <i>Vigna radiata</i> var. <i>radiata</i> | Unknown | RadSA |
| NAM17 | <i>Vigna radiata</i> var. <i>radiata</i> | Unknown | RadSA |
| NAM18 | <i>Vigna radiata</i> var. <i>radiata</i> | Unknown | RadOther |
| NAM19 | <i>Vigna radiata</i> var. <i>radiata</i> | Unknown | RadOther |
| NAM20 | <i>Vigna radiata</i> var. <i>radiata</i> | Taiwan | Admixed_Rad |
| NAM21 | <i>Vigna radiata</i> var. <i>radiata</i> | Unknown | Admixed_Rad |
| NAM22 | <i>Vigna radiata</i> var. <i>radiata</i> | Unknown | RadOther |
| NAM23 | <i>Vigna radiata</i> var. <i>radiata</i> | Pakistan | RadSA |

| | | | |
|--------------|--|-------------|-------------|
| NAM24 | <i>Vigna radiata</i> var. <i>radiata</i> | India | RadSA |
| NAM26 | <i>Vigna radiata</i> var. <i>radiata</i> | Unknown | Admixed_Rad |
| NAM27 | <i>Vigna radiata</i> var. <i>radiata</i> | Unknown | RadOther |
| VI000020AY | <i>Vigna radiata</i> var. <i>radiata</i> | Thailand | RadOther |
| VI000099AG | <i>Vigna radiata</i> var. <i>radiata</i> | India | Admixed_Rad |
| VI000232AG | <i>Vigna radiata</i> var. <i>radiata</i> | Iran | RadOther |
| VI000238AG | <i>Vigna radiata</i> var. <i>radiata</i> | Afghanistan | RadOther |
| VI000542BY | <i>Vigna radiata</i> var. <i>radiata</i> | India | RadSA |
| VI000578AG | <i>Vigna radiata</i> var. <i>radiata</i> | India | RadSA |
| VI000625B-BR | <i>Vigna radiata</i> var. <i>radiata</i> | India | RadOther |
| VI000938AG | <i>Vigna radiata</i> var. <i>radiata</i> | India | RadSA |
| VI001191BG | <i>Vigna radiata</i> var. <i>radiata</i> | Philippines | RadOther |
| VI001435AG | <i>Vigna radiata</i> var. <i>radiata</i> | USA | RadSA |
| VI001509AG | <i>Vigna radiata</i> var. <i>radiata</i> | Pakistan | RadOther |
| VI001514AG | <i>Vigna radiata</i> var. <i>radiata</i> | India | RadSA |
| VI001728AG | <i>Vigna radiata</i> var. <i>radiata</i> | India | RadSA |
| VI001806BG | <i>Vigna radiata</i> var. <i>radiata</i> | Pakistan | Admixed_Rad |
| VI002176BG | <i>Vigna radiata</i> var. <i>radiata</i> | India | Admixed_Rad |
| VI002197BG | <i>Vigna radiata</i> var. <i>radiata</i> | Korea | RadOther |
| VI002239AG | <i>Vigna radiata</i> var. <i>radiata</i> | Afghanistan | RadOther |
| VI002456AG | <i>Vigna radiata</i> var. <i>radiata</i> | Korea | RadOther |
| VI002647AG | <i>Vigna radiata</i> var. <i>radiata</i> | Thailand | RadOther |
| VI002859BG | <i>Vigna radiata</i> var. <i>radiata</i> | Iran | RadOther |
| VI002872BG | <i>Vigna radiata</i> var. <i>radiata</i> | Iran | Admixed_Rad |
| VI002934AG | <i>Vigna radiata</i> var. <i>radiata</i> | India | Admixed_Rad |

| | | | |
|---------------|--|-------------|-------------|
| VI002986AG | <i>Vigna radiata</i> var. <i>radiata</i> | India | RadSA |
| VI003057BG | <i>Vigna radiata</i> var. <i>radiata</i> | India | Admixed_Rad |
| VI003135B-BL | <i>Vigna radiata</i> var. <i>radiata</i> | India | Admixed_Rad |
| VI003255AG | <i>Vigna radiata</i> var. <i>radiata</i> | India | Admixed_Rad |
| VI003337BG | <i>Vigna radiata</i> var. <i>radiata</i> | India | RadSA |
| VI003456AG | <i>Vigna radiata</i> var. <i>radiata</i> | Unknown | RadSA |
| VI003465BG | <i>Vigna radiata</i> var. <i>radiata</i> | India | RadSA |
| VI003480BG | <i>Vigna radiata</i> var. <i>radiata</i> | India | Admixed_Rad |
| VI003534BG | <i>Vigna radiata</i> var. <i>radiata</i> | India | RadSA |
| VI003699B-BR | <i>Vigna radiata</i> var. <i>radiata</i> | India | RadSA |
| VI003894B-BLM | <i>Vigna radiata</i> var. <i>radiata</i> | India | RadSA |
| VI003925B-BLM | <i>Vigna radiata</i> var. <i>radiata</i> | India | RadSA |
| VI003948B-BR | <i>Vigna radiata</i> var. <i>radiata</i> | India | RadOther |
| VI004069BG | <i>Vigna radiata</i> var. <i>radiata</i> | India | Admixed_Rad |
| VI004184AG | <i>Vigna radiata</i> var. <i>radiata</i> | Netherlands | RadOther |
| VI004243B-BR | <i>Vigna radiata</i> var. <i>radiata</i> | Turkey | RadOther |
| VI004244B-BR | <i>Vigna radiata</i> var. <i>radiata</i> | India | RadOther |
| VI004312AG | <i>Vigna radiata</i> var. <i>radiata</i> | India | RadOther |
| VI004432B-BR | <i>Vigna radiata</i> var. <i>radiata</i> | Iran | RadOther |
| VI004666AG | <i>Vigna radiata</i> var. <i>radiata</i> | Iran | RadOther |
| VI004853BG | <i>Vigna radiata</i> var. <i>radiata</i> | India | Admixed_Rad |
| VI004956AG | <i>Vigna radiata</i> var. <i>radiata</i> | Pakistan | RadSA |
| VI004965BG | <i>Vigna radiata</i> var. <i>radiata</i> | Pakistan | Admixed_Rad |
| VI004973B-BLM | <i>Vigna radiata</i> var. <i>radiata</i> | India | RadSA |
| VI005022BG | <i>Vigna radiata</i> var. <i>radiata</i> | India | RadSA |

| | | | |
|------------|--|------------------|-------------|
| VI005030BY | <i>Vigna radiata</i> var. <i>radiata</i> | Mexico | RadOther |
| VI005041AG | <i>Vigna radiata</i> var. <i>radiata</i> | Unknown | RadOther |
| VI014178BG | <i>Vigna radiata</i> var. <i>radiata</i> | Kenya | RadOther |
| VI064196 | <i>Vigna radiata</i> var. <i>radiata</i> | Myanmar | Admixed_Rad |
| VI064197 | <i>Vigna radiata</i> var. <i>radiata</i> | Myanmar | RadSA |
| BCP_075 | <i>Vigna radiata</i> var. <i>sublobata</i> | Papua New Guinea | SubAUe |
| BCP_094 | <i>Vigna radiata</i> var. <i>sublobata</i> | Papua New Guinea | SubAUw |
| CPI_106935 | <i>Vigna radiata</i> var. <i>sublobata</i> | Indonesia | SubTI |
| CPI_107220 | <i>Vigna radiata</i> var. <i>sublobata</i> | Indonesia | SubAUe |
| CQ_1971 | <i>Vigna radiata</i> var. <i>sublobata</i> | Australia | SubAUe |
| CQ_2225 | <i>Vigna radiata</i> var. <i>sublobata</i> | Australia | SubAUe |
| CQ_2226 | <i>Vigna radiata</i> var. <i>sublobata</i> | Australia | SubAUe |
| CQ_2227 | <i>Vigna radiata</i> var. <i>sublobata</i> | Australia | SubAUe |
| CQ_2234 | <i>Vigna radiata</i> var. <i>sublobata</i> | Australia | SubAUe |
| CQ_2238 | <i>Vigna radiata</i> var. <i>sublobata</i> | Australia | SubAUe |
| CQ_2244 | <i>Vigna radiata</i> var. <i>sublobata</i> | Australia | SubAUw |
| CQ_2326 | <i>Vigna radiata</i> var. <i>sublobata</i> | Australia | SubAUe |
| CQ_2649 | <i>Vigna radiata</i> var. <i>sublobata</i> | Australia | SubAUw |
| CQ_2650 | <i>Vigna radiata</i> var. <i>sublobata</i> | Australia | SubAUe |
| CQ_2651 | <i>Vigna radiata</i> var. <i>sublobata</i> | Australia | SubAUe |
| CQ_2733 | <i>Vigna radiata</i> var. <i>sublobata</i> | Australia | SubAUe |
| CQ_2915 | <i>Vigna radiata</i> var. <i>sublobata</i> | Australia | SubAUe |
| CQ_2926 | <i>Vigna radiata</i> var. <i>sublobata</i> | Australia | SubAUw |
| CQ_3066 | <i>Vigna radiata</i> var. <i>sublobata</i> | Australia | SubAUe |
| CQ_3082 | <i>Vigna radiata</i> var. <i>sublobata</i> | Australia | SubAUw |

| | | | |
|-----------|--|------------|----------|
| CQ_3086 | <i>Vigna radiata</i> var. <i>sublobata</i> | Australia | SubAUw |
| CQ_3114 | <i>Vigna radiata</i> var. <i>sublobata</i> | Australia | SubAUe |
| CQ_3233 | <i>Vigna radiata</i> var. <i>sublobata</i> | Australia | SubAUw |
| CQ_3243 | <i>Vigna radiata</i> var. <i>sublobata</i> | Australia | SubAUw |
| CQ_3267 | <i>Vigna radiata</i> var. <i>sublobata</i> | Australia | SubAUw |
| CQ_3269 | <i>Vigna radiata</i> var. <i>sublobata</i> | Australia | SubAUw |
| CQ_3283 | <i>Vigna radiata</i> var. <i>sublobata</i> | Australia | SubAUe |
| CQ_3293 | <i>Vigna radiata</i> var. <i>sublobata</i> | Australia | SubAUw |
| CQ_3323 | <i>Vigna radiata</i> var. <i>sublobata</i> | Australia | SubAUe |
| Karumbyar | <i>Vigna radiata</i> var. <i>sublobata</i> | India | SubAS |
| NAM28 | <i>Vigna radiata</i> var. <i>sublobata</i> | Australia | SubAUe |
| NAM29 | <i>Vigna radiata</i> var. <i>sublobata</i> | Australia | SubAUe |
| NAM30 | <i>Vigna radiata</i> var. <i>sublobata</i> | Indonesia | SubTI |
| TPI_25 | <i>Vigna radiata</i> var. <i>sublobata</i> | Australia | SubAUe |
| VI032155 | <i>Vigna radiata</i> var. <i>sublobata</i> | Australia | SubAUe |
| VI032156 | <i>Vigna radiata</i> var. <i>sublobata</i> | Madagascar | SubAS |
| VI035226 | <i>Vigna mungo</i> | Australia | Outgroup |

- 1 **Supplementary Table S3. Measurement of seed weight in wild accessions from genetic**
- 2 **groups of SubAU and SubAS.** The data are presented as mean \pm standard error.

| Accession | Genetic group | Seed weight (mg/100 seeds) | Seed number (seeds/pod) | Pod length (cm) |
|------------------|----------------------|-----------------------------------|--------------------------------|------------------------|
| CQ2234 | SubAU | 1491.82 \pm 39.18 | 7.83 \pm 0.2 | 4.06 \pm 0.06 |
| NAM30 | SubAU | 1198.19 \pm 63.64 | 9.63 \pm 0.27 | 3.74 \pm 0.06 |
| CQ3267 | SubAU | 1808.12 \pm 58.44 | 7.87 \pm 0.33 | 4.54 \pm 0.12 |
| Karumbyar | SubAS | 2775.46 \pm 106.63 | 11.87 \pm 0.23 | 5.63 \pm 0.08 |
| VI032156 | SubAS | 2176.56 \pm 209.72 | 9.53 \pm 0.32 | 5.47 \pm 0.09 |

3

Supplementary Table S4. List of GPS sites of wild mungbeans used for niche modeling

| Region | Longitude | Latitude | Source |
|---------------|------------------|-----------------|---------------|
| South Asia | 71.397 | 25.752 | NBPGR |
| South Asia | 73.312 | 28.023 | NBPGR |
| South Asia | 73.312 | 16.99 | NBPGR |
| South Asia | 73.383 | 18.75 | NBPGR |
| South Asia | 73.559 | 21.876 | NBPGR |
| South Asia | 75.303 | 22.601 | NBPGR |
| South Asia | 76.071 | 11.051 | NBPGR |
| South Asia | 76.214 | 10.528 | NBPGR |
| South Asia | 76.655 | 10.787 | NBPGR |
| South Asia | 76.956 | 11.017 | NBPGR |
| South Asia | 77.103 | 9.919 | NBPGR |
| South Asia | 77.167 | 19.817 | GBIF |
| South Asia | 78.767 | 15.417 | GBIF |
| South Asia | 78.883 | 12.867 | GBIF |
| South Asia | 79.017 | 11.417 | AGG |
| South Asia | 79.017 | 11.433 | GBIF |
| South Asia | 79.986 | 23.182 | NBPGR |
| South Asia | 80.017 | 17.817 | GBIF |
| South Asia | 80.067 | 23.067 | GBIF |
| South Asia | 80.167 | 17.55 | GBIF |
| South Asia | 81.067 | 17.717 | GBIF |
| South Asia | 81.883 | 18.344 | NBPGR |

| | | | |
|----------------|---------|--------|------|
| Southeast Asia | 100.673 | -0.322 | GBIF |
| Southeast Asia | 107.009 | -6.741 | GBIF |
| Southeast Asia | 106.791 | -6.59 | GBIF |
| Southeast Asia | 107.005 | -6.738 | GBIF |
| Southeast Asia | 107.621 | -6.913 | GBIF |
| Southeast Asia | 108.211 | -7.654 | GBIF |
| Southeast Asia | 109.923 | -7.187 | GBIF |
| Southeast Asia | 114.133 | -8.083 | GBIF |
| Southeast Asia | 106.978 | -6.703 | GBIF |
| Southeast Asia | 120.338 | 23.235 | GBIF |
| Southeast Asia | 121.514 | 22.056 | GBIF |
| Southeast Asia | 120.822 | 24.253 | GBIF |
| Southeast Asia | 120.848 | 21.903 | GBIF |
| Southeast Asia | 121.53 | 25.008 | GBIF |
| Southeast Asia | 120.871 | 24.271 | GBIF |
| Southeast Asia | 120.202 | 22.989 | GBIF |
| Southeast Asia | 120.669 | 22.344 | GBIF |
| Southeast Asia | 120.282 | 22.628 | GBIF |
| Southeast Asia | 120.321 | 22.823 | GBIF |
| Southeast Asia | 98.7 | 19.117 | GBIF |
| Southeast Asia | 98.733 | 19.2 | GBIF |
| Southeast Asia | 98.783 | 18.95 | GBIF |
| Southeast Asia | 99.217 | 18.333 | GBIF |
| Southeast Asia | 99.833 | 20.3 | GBIF |
| Southeast Asia | 99.867 | 18.333 | GBIF |

| | | | |
|---------------------|---------|---------|------|
| Southeast Asia | 101.063 | 13.254 | GBIF |
| Southern Hemisphere | 120.167 | -1.167 | AGG |
| Southern Hemisphere | 152.55 | -27.117 | AGG |
| Southern Hemisphere | 152.583 | -26.517 | AGG |
| Southern Hemisphere | 148.167 | -23.667 | AGG |
| Southern Hemisphere | 148.15 | -22.233 | AGG |
| Southern Hemisphere | 149.25 | -21.5 | AGG |
| Southern Hemisphere | 148.383 | -21.133 | AGG |
| Southern Hemisphere | 119.667 | -20.833 | AGG |
| Southern Hemisphere | 144.3 | -18.667 | AGG |
| Southern Hemisphere | 146.165 | -18.581 | AGG |
| Southern Hemisphere | 125.383 | -18.083 | AGG |
| Southern Hemisphere | 127.8 | -18.033 | AGG |
| Southern Hemisphere | 122.253 | -17.781 | AGG |
| Southern Hemisphere | 122.209 | -17.706 | AGG |
| Southern Hemisphere | 145.5 | -17.017 | AGG |
| Southern Hemisphere | 129.151 | -16.866 | AGG |
| Southern Hemisphere | 125.933 | -16.717 | AGG |
| Southern Hemisphere | 131.2 | -16.367 | AGG |
| Southern Hemisphere | 133.05 | -16.217 | AGG |
| Southern Hemisphere | 130.383 | -15.633 | AGG |
| Southern Hemisphere | 145.25 | -15.483 | AGG |
| Southern Hemisphere | 128.117 | -15.467 | AGG |
| Southern Hemisphere | 131.733 | -15.067 | AGG |
| Southern Hemisphere | 131.183 | -13.833 | AGG |

| | | | |
|---------------------|---------|---------|-----|
| Southern Hemisphere | 132.32 | -12.554 | AGG |
| Southern Hemisphere | 131.05 | -12.533 | AGG |
| Southern Hemisphere | 136.883 | -12.25 | AGG |
| Southern Hemisphere | 123.633 | -10.217 | AGG |
| Southern Hemisphere | 123.567 | -10.167 | AGG |
| Southern Hemisphere | 124.167 | -10 | AGG |
| Southern Hemisphere | 124.567 | -9.517 | AGG |
| Southern Hemisphere | 124.5 | -9.483 | AGG |
| Southern Hemisphere | 124.77 | -9.45 | AGG |
| Southern Hemisphere | 143.42 | -9.007 | AGG |
| Southern Hemisphere | 126.3 | -7.7 | AGG |
| Southern Hemisphere | 134.333 | -6.75 | AGG |
| Southern Hemisphere | 146.997 | -6.738 | AGG |
| Southern Hemisphere | 146.717 | -6.583 | AGG |
| Southern Hemisphere | 144.933 | -4.267 | AGG |

4

5

6 **Supplementary Table S5. List of primers used in this study**

| Primer | Sequence | Target gene |
|-----------------|--------------------------------|--------------------|
| Vrdet1-P3-F | GGCAAGAATGCCTTTGGAACC | <i>VrDet1</i> |
| Vrdet1-P3-R | AGCATCTGTTGTGCCTGGAA | <i>VrDet1</i> |
| VrMYB26-qPCR-F2 | GGTTGCTGGAGTTCCGTCCCAAAA | <i>VrMYB26a</i> |
| VrMYB26-qPCR-R | AACCATTGGCAAGACCGTGA | <i>VrMYB26a</i> |
| CYP20-F | TCCCCAAACAGCCGAAAA | <i>VrCYP20</i> |
| CYP20-R | CCCCTTGAATCATGAAATCCTT | <i>VrCYP20</i> |
| VrCAD4-cDNA-F2 | CCTACAATCTAAGAAACACTGGCCCTGATG | <i>VrCAD4</i> |
| VrCAD4-cDNA-R2 | AACTACCTCGTGTCCGGGGA | <i>VrCAD4</i> |

7

8

9